A System Design for the MRO Interferometer

Revision: 1.31 Date: October 2002

Contents

1 Introduction

The following is a working draft of a system design for the Magdalena Ridge Observatory Interferometer. It attempts to proceed from a set of well-defined science goals to an implementation which is capable of meeting these science goals within the resources available. The presentation is mostly in the form of top-down design, even though the actual design process has been an iterative one in which the top-level requirements have been changed in the light of implementation constraints.

This document is of necessity incomplete since it represents a work in progress, and some parts of the design have not reached the same state of maturity as other parts of the design. Those items covered in detail have been considered in some depth, but where possible we have attempted to highlight areas that require further study. In many cases a final decision has not been made on the direction to take in a given design, but what is presented is either a set of design choices or a route towards making the design choice. Some attempt has been made to ensure that the different parts of the design are at least consistent with one another, but this has not been always been possible.

2 Aims and objectives

For the purposes of this document we have assumed that funding is available to build an interferometer at the Magdalena Ridge Observatory (MRO) in New Mexico. Hereafter we will call this interferometer the MROI. Discussion of other developments on this site, e.g. a fast-tracking single dish telescope, is left to other documents and will not be considered further here.

2.1 Strategic aims

The context for the MROI is principally determined by a number of other large interferometric projects that are underway at present. These are summarized in the table below, where we have made what we feel are reasonable assessments of where these projects will be on the timescale for initial operations with the MROI.

Facility & location	N	$D/$m	$B/$m	Primary operational roles in 2005+
CHARA: Mt. Wilson, USA	6	1.0	350	Optical and near-IR imaging
ISI: Mt. Wilson, USA	3	1.7	85	$10\,\mu$m astrophysics
NPOI: Flagstaff, USA	6	0.5	440	Optical astrometry and imaging
SUSI: Narrabri, Australia	2	0.1	640	Optical visibilities
KECK: M. Kea, Hawaii	$2+4$	$10.0+1.8$	140	Near-IR astrometry and $10\,\mu$m visibilities
VLTI: Paranal, Chile	$4+3$	$8.0+1.8$	200	Near-IR astrometry and $10\,\mu$m visibilities

Table 1: Major optical/infrared astronomical interferometer arrays. In this summary only major facility instruments which we expect to be operating in the 2005+ time-frame are included. N, D, and B refer to the number of telescopes in the array, their aperture size, and the maximum baseline achievable. Both the Keck and VLTI arrays have the possibility of using a mixture of large and more modestly sized telescopes. All figures are approximate.

While the primary operational roles of the arrays in Table 1 span a broad range of capability, it is noticeable that none of them combines large numbers of $1\,$m-class collecting apertures. With this background in mind, the basic aims for the MROI have been established as follows:

- That it be a unique, world class interferometer array. A principal feature of the array must be an ability to undertake important and topical science programmes that other arrays are unable to pursue.

- That it have a broad rather than specialist science remit. This is required so as to attract support from a wide community both in the US and the UK, and is likely to be a necessity for securing support for the continued operation and maintenance of the array once it has been commissioned.

- That it advance education in New Mexico. To do this it must deliver "spectacular" science so as to attract and enthuse both student and general public audiences. It should also allow for the training and development of undergraduate and graduate scientists, both to support the astronomical facilities and research programs in New Mexico, and to provide a pool of skilled technical personnel for the wider labor market.

- To further the US Navy's strategic goals it must also provide the capability to investigate combining adaptive optics with interferometry.

2.2 Science objectives

To meet these aims, we have developed a preliminary science case which is detailed in an appendix to this document. Scientists from over a third of the Astrophysics Departments in the UK contributed

towards this overview, and their number gives some indication of the range of possible applications of interferometric imaging to contemporary astrophysics. Their initial document was augmented with additional programmes that further matched the interests of astronomers in New Mexico. A key feature of the resulting case is that it demonstrates the breadth of science possible with an interferometer whose sensitivity, angular resolution and imaging capability are appropriately chosen. The broad remit of the case covers three primary topical branches of astrophysics:

1. **Active galactic nuclei:** resolved imaging of the nuclear dust component of AGN, the broad-line-region (BLR), synchrotron jets and nuclear and extra-nuclear starbursts.

2. **Stellar accretion and mass loss:** via winds, jets, outflows, and Roche-lobe overflow. Studies of examples in single and binary systems in themselves and as analogs for AGN jets and beams.

3. **Star and planet formation:** the detection and characterization of protostellar disks. Accretion, disk-clearing, fragmentation and stellar duplicity over all mass ranges. Stellar rotation in clusters and angular momentum distribution.

3 Overall concept

To address the three primary science missions outlined above, i.e. studies of active galactic nuclei, stellar accretion and mass loss, and star and planet formation, our overall design concept for the Magdalena Ridge Observatory Interferometer is that of a state-of-the-art facility imaging array. A critical assessment of existing interferometric arrays suggests that the principal distinguishing feature of the MROI will be its ability to image *faint* and *complex* sources in a model-independent manner. This capability has been singularly lacking from the current generation of optical/infrared interferometers, and it has undoubtedly been the major stumbling block to optical/infrared interferometry being championed by the broad astronomical community.

Within this framework the major features we envisage for the MROI can be broadly described as follows. For information, brief statements of the technical and scientific drivers for these are included below as well:

- A basic unit-telescope size large enough to provide the **sensitivity** to permit fringe tracking on reasonable samples of all of the primary targets defined in the top-level science mission.

- An approach to **adaptive optics** that satisfies the desire to explore the combination of interferometry with adaptive optics beyond tip and tilt. We expect this to be pursued with the goal of impacting only positively on the top level science mission of the MROI.

- Coverage in **wavelength** so as to allow imaging in key optical diagnostic lines and with access to the photometric bands in which the top-level science targets are bright and where the best interferometric sensitivity can be realized.

- A **spectroscopic** capability that allows useful isolation of atomic lines and molecular features from their nearby continuum in stellar sources, and velocity resolved imaging in the very nearest AGN.

- An **interferometric field-of-view** to allow imaging across a single primary beam of the unit telescopes, when bandwidth constraints allow this. Larger fields of up to ± 1 arcsecond may be accommodated without replacement of the beam relay optics, but are not required for the targets identified in the current version of the science case and would require a specialized beam combiner.

- A choice of **interferometric baselines** matched to the full range of science targets in the top-level science mission. This requires a reconfigurable array, with movable telescopes, and a probable mode of operation where the array configuration is adjusted as required, similar to what is performed for the VLA. The array should have a **low-resolution** configuration to allow comparison of its interferometric observations with complementary data from facilities such as HST, ALMA, NGST, Keck AO etc.

- A sufficient **number** of telescopes so as to allow at least 5×5 pixel model-independent imaging for fully resolved objects. For sources with a strong unresolved component, images as large as 10×10 pixels should be achievable. Since many of the sources identified in the top-level science mission evolve on monthly or weekly timescales, the number of telescopes must be sufficient to allow imaging without relocation of the array elements.

- A level of **automation and reliability** to allow exploitation of the times of best seeing for the most challenging astronomical projects, and to minimize overall staffing and running costs. The large numbers of replicated subsystems in the array make this a far more demanding task than for a single telescope observatory.

- An **operational model** that envisages only facility service observing. Trained telescope operators would run the array, overseeing the automated sequencing of observations with minimal intervention.

- A **scientific prioritization** that identifies the delivery of model-independent imaging of faint sources as a mandatory requirement for the MROI in its first phase of operation. Other capabilities, such as polarimetry and wide-field imaging should be accommodated where possible.

- An overall **technical design philosophy** that allows for potential expansion in basic capability in the longer term. We expect that additional technical capabilities will be added to the array on the basis of maintaining its position as a world-class astronomical facility. One good example of this is a polarimetric capability, where we would not wish to restrict future development of this area if it became a focus in the longer term.

In summary, our concept for the MROI is a reconfigurable multi-element moderate-sized aperture optical/infrared interferometer. Its primary function will be to deliver reliable imaging of faint and complex astronomical targets. We believe that this deliverable alone can realistically be expected to engage the public, politicians, funding agencies and the wider astronomical community, all of whom will be needed to support the MROI beyond its initial commissioning phase. Exactly how this can be achieved will be explored in the following section.

4 Functional requirements

The goals highlighted above imply a number of overall design parameters which are summarized below and expanded on in later sections of this report. While later sections of this document divide the array into a number of subsystems, many of the arguments relating specific parts of the design to specific requirements necessarily cross subsystem boundaries. As a result in some cases the justification for a particular design feature refers both forwards and backwards within the document.

4.1 Sensitivity

The extra-galactic component of the top-level science mission for the MROI sets the basic requirement for its desired sensitivity. At K-band magnitudes fainter than about 11 the very closest and brightest active galactic nuclei just start to become visible. However, it is not until a K-band sensitivity of 14 is reached that of order 100 targets become visible in the Northern celestial sky. This is a large enough sample that even if as many as 75% of these sources are too large to be studied interferometrically a large enough number of sources amenable to detailed study will remain. It is worth noting that at this limiting sensitivity many tens to hundreds of examples of *all* of the sources categories enumerated in the top-level science mission will be observable. For example at a K magnitude of 14 all condensed sources down to the hydrogen burning limit will be detectable at the distance of the Taurus-Auriga star forming region.

As will be expanded on later, the concept of sensitivity for an optical/infrared interferometer has a very precise meaning. In particular, what we mean by a "sensitivity" of 14th magnitude in a given band is that some form of fringe tracking — either phase or envelope tracking — be possible with a source of that brightness. Once the interferometer is stabilized against the atmospheric fluctuations in this manner, science observations at much lower light levels can be made in bandpasses not being used for the fringe tracking.

In practice, this sensitivity requirement for the array is particularly challenging and will require careful attention to detail at all stages of the array design. Most important will be the optimization of throughput and wavefront quality along the whole optical train. The analysis presented in the subsequent section of this report shows that this top-level sensitivity requirement can be met with unit telescopes employing tip-tilt correction with an aperture diameter of $1.4\,\mathrm{m}$ when the seeing is better than 0.75 arcseconds by tracking the atmospheric fluctuations in the H-band. The reduction in thermal background in going from $2.2\,\mu\mathrm{m}$ to $1.65\,\mu\mathrm{m}$ is sufficient to allow existing near-infrared detectors to be used to achieve this goal, and thus eliminates one of the few major risk elements associated with the array subsystems.

4.2 Wavelength range

From an astronomical perspective most scientists would agree that the MROI should attempt to exploit as broad a range of wavelengths as possible, perhaps from the ultraviolet at $350\,\mathrm{nm}$ to the mid-infrared at $10\,\mu\mathrm{m}$. However, many years of experience with existing interferometric arrays has made clear that at short wavelengths the rapid deterioration in r_0 and t_0 means that it is essentially impossible to compensate for the atmosphere usefully. Similarly, towards the mid-infrared it is well established that the huge thermal background forces the use of very large collecting apertures if good sensitivity is to be achieved.

With these boundary conditions in mind, we are proposing a top-level design goal that the MROI operate between 0.6 and $2.4\,\mu\mathrm{m}$. This will allow observations at H-α, a key line for active galaxies and other energetic sources, but will also give access to the K-band which will be crucial for penetrating dust in AGN and YSOs. Unless aperture sizes comparable to those being use for mid-infrared observations at the Keck and VLTI arrays are envisioned, there is no compelling scientific case for extending this range to longer wavelengths. Measurements at wavelengths shorter than $0.6\,\mu\mathrm{m}$ should be explored on

a best-effort basis. i.e. with due regard to not compromising the array's capabilities between 0.6 and $2.4\,\mu$m.

In practical terms, the wide wavelength range required for the array means that the coatings along the optical train will need to have excellent broadband amplitude and phase performance. Furthermore, it is likely that the majority of the optics should be reflective. If existing technologies are to be used, then at least two types of detector types will be needed.

4.3   Spectroscopic resolution

The spectroscopic resolution of the MROI that we are proposing is fairly straightforwardly set by the type of astronomical programmes we have in mind. Faint source imaging will require rather broad continuum bandpasses, while studies of spectral features in active and interacting stars will need to resolve the line profiles. We thus envisage the spectroscopic back-ends of the beam combining assemblies to have multiple user-selectable dispersing elements. As a first step, spectral resolutions of no greater than a few hundred will be adequate for studies of, for example, molecular features in cool stellar atmospheres and broad emission lines in active galaxies. However, this will need to be coupled with a mode with a resolution perhaps ten times higher (e.g. $R \simeq 5000$) for velocity resolved measurements of Doppler broadened lines in stellar ejecta, and possibly a higher resolution mode (e.g. $R \simeq 30000$) for certain stellar rotation studies.

4.4   Spatial resolution

The scientific scope of the MROI is sufficiently broad that the range of angular scales of interest to its users will be very large. On the smallest scales, accretion streamers onto protostars in even the nearest star forming regions will be expected to subtend angles of no more than a few tenths of a milliarcsecond. Similarly, the broad line regions of the brightest active galactic nuclei might be expected to have a similar scale size. On the other hand, the dust ejecta from the brightest supergiant and giants stars has already been detected on scales of many tens of milliarcseconds, and so one should expect numerous sources subtending angles of order several milliarcseconds.

These angular scales transform straightforwardly to maximum baselines ranging from 50 m for the largest sources to 500 m for the smallest, and can clearly only be accommodated with some sort of reconfigurable array. While the very highest angular resolution would be desirable at some stage, one possible scenario would be to operate with minimum baselines as short as ~ 10 m and a maximum baseline of order 300 m in a first phase of operation. Further extensions to the array could then be added as and when the opportunity and interest arose.

4.5   Imaging and number of telescopes

The quality of imaging required for the primary science programmes has been assessed by examining existing interferometric images from prototype arrays, and asking whether or not they would be useful in discriminating between competing models for any given science programme. The result of this analysis is that images with 5×5 pixels must be achievable, and for brighter sources, images with as many as 10×10 pixels would be desirable. Both of these goals should be achievable without array reconfiguration.

These types of image require that for any configuration of the array a 5:1 (or 10:1) ratio of baseline lengths be available. This could be realised with, for example, a 6-element linear non-redundant array, but this type of arrangement would likely not allow for baseline-bootstrapping. A preferable approach is to use a quasi-redundant array with a larger number of array elements. When combined with the need to deliver a "snapshot" imaging capability — this will be particularly important for time variable sources — this implies of order 10 array elements in a two-dimensional layout. Smaller numbers of telescopes in a 2d configuration are unlikely to be able to satisfy the top-level science requirements.

Another important aspect of the imaging that is delivered is its dynamic range, i.e. the ratio of the brightest and weakest believable features in any recovered maps. For bright sources, the limit on the dynamic range will be determined by the fractional error $\delta A/A$ and the phase error $\delta \phi$, on the individual visibility amplitudes and phases, and their total number, n. As a rough guide, the dynamic range will be given by

$$\frac{\sqrt{n}}{\sqrt{\left[(\delta A/A)^2 + (\delta \phi)^2\right]}} \;.$$

Whilst errors on the visibility amplitudes of less than 1 per cent are certainly achievable, phase errors may well be as large as 2 degrees, i.e. 3 percent of a radian, and hence be the dominant factor. For a 10-element array, the number of separate visibilities will easily be of order 200, and 2000 is perhaps more realistic for a night-long observation. These figures thus give a dynamic range of approximately 1000 : 1, some 10 times better than has been realized in the best interferometric maps to date, and allowing for the detection of sources 7.5 magnitudes fainter than any bright core in an image.

4.6 Automation

It is well established that the most productive optical/infrared interferometers have been those with highly automated sequencing and operation. Our design philosophy for the MROI implicitly assumes this model, so that tasks such as pre-observing alignment of the optical trains, self-testing of the detector and beam combination subsystems, and failure recovery, will all be carried out transparently with a minimum of operator intervention.

The large numbers of replicated subsystems in the array also implies a high premium on the reliability and fault-tolerance of the array as a whole. As a result we expect considerable design effort to be expended on a control architecture that allows for remote diagnostic testing of hardware and a hardware model that permits rapid modular exchange of defective systems.

4.7 Observing

Like most other radio and optical interferometers, the operational model we envisage for the MROI is that of service observing, i.e. a situation where observers prepare and submit proposals remotely and where successful observing programmes are executed by a team of dedicated operators. This implies no need for observer accommodation on site, but that a small staff of operators skilled at running and overseeing the observations are present.

The positive implications of this approach are basically twofold. It will allow much more control of the scheduling of observations, and hence improve the efficiency of operations. And second, it is likely to lead to considerable savings in manpower and running costs as compared to a conventional observatory where instrument changes might take place much more frequently. It will, of course, necessitate the development of pre-observing software tools, an automated data reduction pipeline, and a distribution mechanism for the final calibrated data.

4.8 Scientific scope

It is perhaps worth ending this section by reiterating the intimate connection between the functional specification we have just outlined and the top-level science goals for the MROI. In particular the precise rationale for three key features of the array deserve special mention:

- Angular resolution: where the range of angular scales of interest has driven the specification and implies a reconfigurable array with both very short and very long baseline configurations. No other array will be able to match the MROI.

- Imaging fidelity: where the number of baselines observable simultaneously, i.e. the "snapshot" capability of the array, has been prioritized. With a minimum of 10 elements the MROI will be able to image faster and more reliably than any other array with a dynamic range a factor of 10 better than has been achieved to date.

- Sensitivity: where the combination of moderately large collector sizes ($\sim 1.4\,\mathrm{m}$ diameter) and an optical train simultaneously optimized for throughput and wavefront quality will lead to unprecedented performance.

While it may seem that these three key functions are merely incremental enhancements on what has been achieved before, it is the combination of all three in a single interferometer that will make the MROI truly unique scientifically. And it is their combination in an integrated and coherent whole, rather than any specific technical hurdle, that probably represents the real challenge for the project.

5   The site

The site chosen for the Magdalena Ridge Observatory is adjacent to the Langmuir Laboratory for Atmospheric Research, at a latitude of 34 degrees and at a height of 3220m, where the air pressure is only 0.7 of the sea-level value. A saddle point near the summit allows a Y shaped array with baselines of more than 300 m and ample space for an appropriate delay-line building of an approximate length of 200 m.

The MRO site development programme is the subject of a new Environment Impact Statement to cover the changed use of the site, and we expect this may take a year to complete. No substantial work can take place on the site until it is complete and a new agreement signed with the Forestry Service.

5.1   Seeing

The atmospheric seeing at MRO will play a crucial role in setting the limiting performance of the interferometer. It is conventionally characterized by 2 quantities — a spatial scale r_0 (Fried's parameter) and a temporal scale t_0, the coherence time.

A number of measurements of the spatial scale at the Magdalena Ridge already exist which show sub-arcsecond seeing, corresponding to values of r_0 greater than 10cm at visible wavelengths. The coherence time has currently not been measured, but it can be estimated on the usual assumption that the turbulence behaves as a fixed phase screen blown passed the telescopes by a wind of known speed. This coarse analysis gives values of t_0 of 3 milliseconds for the typical wind speed of 5 meters per second.

We are currently assessing other recent measurements of r_0 at various locations on the site. Near-simultaneous measurements at a number of different locations show the same behavior, with values for the seeing of between 0.6 and 1 seconds of arc.

We will start making seeing measurements on a regular basis in October at the JOCR building. Eventually we would like to do more measurements down at the array site. We need to get a second Differential Image Motion Monitor (DIMM) system for that. Trials of the Cambridge DIMMWIT seeing monitor, which can measure t_0 as well as r_0, planned for November 2002 and spring 2003.

In the longer term we will purchase a complete fully automated DIMM telescope that would become the standard system for the mountain (8 - 10 months for delivery). It would be put in the JOCR building until we can determine the best place to put it on the mountain and we get past the environmental approvals.

Only after accurate measurements throughout the year, will prediction of the normal and best performance of the interferometer be possible.

5.2   Weather

There is a large archive of weather data for the site, as a detailed site survey was done for the mm array programme. The annual mean wind speed is 8.6 mph, with stronger winds of 12mph in February. There is snow at the site frequently. The design of the telescopes and their covers must cater for these varied conditions and reasonable extreme values.

The transparency is very good. This is good news though not crucial for the performance of our interferometer. We believe that useful observing will be possible on about half the nights of the year. Sixty nights will be lost to bad weather, 60 to high wind, 30 to maintenance, and 60 will have thin cloud, leaving 155 nights with high quality conditions. Note that the 60 nights with thin cloud will still be usable for programmes on brighter sources and for technical programmes. There is wetter weather in July, August, and September during the "monsoon" and this will undoubtedly affect the way observing is programmed.

The Langmuir Laboratory is sited here, in part, because of the high incidence of thunderstorms (about 1 per day in July and August). We will take advice from experts about minimising the risks

of damage to the telescopes and their electronics. This clearly possible, since the VLA is within sight and operates successfully under very similar conditions.

We plan to have our own weather station in operation at the site, in a couple of months. We may need an "all sky camera", IR or a visual one, to warn of impending changes in weather conditions.

5.3   Seismic issues

Interferometers are vulnerable to seismic activity, as it may reduce the fringe contrast or make building a usable instrument very difficult. However, currently there is no reason to believe the site presents problems.

To assist, particularly in the design of foundations, we need data on the normal background level of movement on various timescales (10ms, 24hr and monthly). Also we need data on the rate of occurrence of major seismic events.

We are planning on putting in 4 seismic stations at the site: one in the middle of the array and 3 others, one at the ends of each arm of the array. We have Forest Service approval for this and expect to hire a graduate student from Geophysics to work on the data for about 1 year commencing very soon.

It should be remembered that like any interferometer we are only sensitive to differential movements, and so this means that even an active site may be suitable for an array of moderate size.

6   Error budgets

As mentioned earlier, the most demanding requirement placed on the array design will be that associated with its sensitivity. It is crucially important to note that because interferometers are fundamentally limited by the number of photons that can be collected in an r_0-sized patch during a time t_0 any sensitivity lost through poor design *cannot* be recovered by simply increasing the telescope diameter or the integration time.

In this version of the document we thus consider an error budget which is entirely driven by signal-to-noise ratio criteria. Other criteria may be added later.

6.1   The interferometric signal-to-noise ratio

The most convenient and appropriate model for the interferometer here is that at its most basic level it collects a sequence of "exposures" of fringe patterns, each with some integration time which we will refer to hereafter as the "coherent integration time". These data can then be averaged incoherently by means of the power spectrum (to get the visibility modulus) or the bispectrum (to get the closure phase) to get an increased SNR. The incoherent integration time can in principle be increased indefinitely by repeating the observation at the same sidereal time (to get the same projected baseline) on many nights in succession. Hence, there is no *fundamental* limit to the SNR of a visibility modulus or closure phase measurement as long as the source does not change over the timescale of the measurements.

However, the presence of the Earth's atmosphere affects this argument. In particular, the Earth's atmosphere perturbs the differential paths to the array elements by many tens of microns on timescales of a few seconds. If no attempt is made to follow these path fluctuations it is likely that no fringes will be seen for most exposures since the differential paths will be much greater than the coherence length of the light being measured. Active acquisition and tracking of the interferometer fringes is therefore a necessary condition for the interferometer to work at all!

This tracking relies on being able to derive a path-error signal with a suitable SNR on a timescale less than the timescales on which the atmosphere moves the fringes out of view. So, if there are too few photons available to do the fringe tracking, or the fringes have too low a contrast, the source simply cannot be observed. This will be independent of how much observation time is available. In short, the fundamental sensitivity limit of the interferometer will be set by the signal-to-noise ratio for fringe tracking.

In the photon-noise-limited regime, the SNR of all fringe tracking schemes is essentially a monotonic function of $< V^2 > N$ where $< V^2 >$ is the mean-squared apparent fringe visibility and N is the mean number of photons received in a coherent integration time. Because the dependence on V is quadratic, more stringent requirements must be set on the apparent fringe contrast than on the photon throughput.

6.2   Global wavefront error

Aberrations introduced by the Earth's atmosphere will reduce the fringe contrast by an amount which depends on the aperture size used and the coherent integration time. Any extra spatial aberrations and pathlength fluctuations introduced by the interferometer optics will further reduce V.

If the interferometer optics introduce random wavefront aberrations with an rms value of $\sigma_{\mathrm{spatial}}$ radians into the light from each telescope, the resulting fringes will have a visibility reduction of approximately $\exp(-\sigma_{\mathrm{spatial}}^2)$. Similarly, if fluctuations in the internal paths inside the interferometer introduce an rms phase jitter of $\sigma_{\mathrm{temporal}}$ radians into each beam during a coherent integration time, the contrast will also be reduced by a factor of $\exp(-\sigma_{\mathrm{temporal}}^2)$. Thus, if the interferometer optics introduce spatial aberrations at the level of $\sigma_{\mathrm{spatial}} = \lambda/14$ and a temporal piston jitter of $\sigma_{\mathrm{temporal}} = \lambda/14$ then each of these two effects will introduce a reduction in the observed visibility by a factor 0.8, which is the same as introduced by the atmosphere over a tip-tilt corrected aperture of diameter $1.5r_0$ or

during an integration time of $1.7t_0$. We adopt these as the error budgets for the entire interferometer, with the exclusion of the fast tip-tilt system. For the latter we adopt the requirement that any residual errors in tilt-correction should lead to a visibility loss of no more than 10%.

The telescope optics will be the largest elements in the optical train and also the only articulated optics and so it seems prudent to allocate half of the total spatial wavefront error budget to the telescopes alone. This leads to a constraint on the telescope optics errors of $\sigma_{\mathrm{spatial}} = \lambda/20$ and $\sigma_{\mathrm{temporal}} = \lambda/20$, and the same constraint on the rest of the system. We will define the telescope optics as the train of optics the astronomical beam sees when going from the sky until it begins travelling in a direction which is fixed with respect to the Earth's surface.

6.2.1 Wavelength dependencies

These wavefront error tolerances will be most difficult to realize at the shortest wavelength the system must work at, i.e., at 600 nm in this case. However, these constraints will be relaxed somewhat because the useful system aperture size and integration time will be smaller at these shorter wavelengths.

The reason for this is as follows. It is well established that in presence of atmospheric fluctuations there are optimal values for the telescope diameter and coherent integration time that maximize the SNR of the fringe measurements. These are roughly 2–$3{\times}r_0$ for a tip-tilt-corrected telescope aperture and 1–$2{\times}t_0$ for the integration time, where r_0 is Fried's parameter and $t_0 = 0.314 r_0/v_{\mathrm{wind}}$ is the atmospheric coherence time.

Since r_0 and t_0 both increase as $\lambda^{6/5}$, apertures and integration times which are optimal at longer wavelengths will be too large at shorter wavelengths. This is remedied by stopping down the aperture and reducing the integration time when observing at shorter wavelengths. As a result, the spatial and temporal scales over which a given wavefront tolerance must be met reduce for shorter wavelengths. For example, if $r_0 = 13$ cm at $\lambda = 500$ nm, a $3r_0$ aperture corresponds to 49 cm at $\lambda = 600$nm and 231 cm at $\lambda = 2200$nm. For $t_0 = 4$ ms at $\lambda = 500$ nm, a $2t_0$ integration time corresponds to 10 ms at $\lambda = 600$nm and 50ms at $\lambda = 2200$nm. These figures will be used as the appropriate apertures over which the tolerances need to be met at each wavelength.

6.3 Throughput

A goal for the interferometer is to have 20% throughput from the sky to detected photons. At the COAST array in Cambridge, the throughput from sky to detected photons has been measured to be $\sim 4.3\%$ at a wavelength where the detector quantum efficiency is 29 percent. Replacement with a Rockwell FPA with a quoted efficiency of 70% would thus give the COAST system a throughput of 10%. At COAST we have not seriously attempted to optimize the array throughput and so a goal of 20% for the MROI does not seem unreasonable.

For a system with surfaces whose average reflectance is 0.95, a final detector with a quantum efficiency of 70%, and assuming a sky transparency of 80%, no more than 20 surfaces can be allowed in total from the sky to the detector.

6.4 Limiting magnitude

We calculate here whether the proposed interferometer will be able to observe the faint sources which are of scientific interest. We will take as a test case the observation of an AGN with an unresolved core magnitude of $H = 14$ and $V = 16$. Whether fringe data can be taken on a faint source will be set by two factors. Firstly if the fringe tracker does not have enough light to track fringes then the source cannot be observed. Secondly, if the tip-tilt or AO system does not have a sufficiently high SNR in the wavefront sensor to adequately correct the wavefront then the fringe contrast will be reduced and so the fringe-tracker SNR may be reduced below a level where fringe tracking is possible. We will examine these two requirements below.

6.4.1 Assumptions

For the purposes of this section we assume an interferometer with 1.4 meter diameter apertures with tip-tilt correction only. We assume that the interferometer achieves the stated design goals so that the system throughput from the sky to detected photons is 20% and that the degradation in fringe contrast due to spatial wavefront errors in the interferometer is 0.8, that the degradation due to temporal phase jitter is 0.8 and that the degradation due to imperfect tip-tilt tracking is 0.9, leading to a total degradation by a factor of 0.57. We further assume that the interferometer operates a group-delay fringe tracker which tracks the fringe envelope using all of the H-band light with a center wavelength of 1.65μm and a bandpass FWHM of 0.3μm. The fringe tracker uses a pairwise combiner with 5 spectral channels and a detector with read noise $\sigma = 1.5$ electrons. It is to be noted that this read noise specification is an ambitious one, and is discussed further in the detectors section. The seeing is assumed to be $r_0 = 14$cm and $t_0 = 4.2$ms measured at $\lambda = 500$nm.

The tip-tilt system is assumed to use all the light in the B and V bands across the whole aperture to do the wavefront sensing. The throughput from the sky to detected photons in the tilt sensor is assumed to be 30%.

Both the fringe tracker and tip-tilt sensor are assumed to use an on-axis source for wavefront sensing.

6.5 Fringe-tracking SNR

For a set of pair-wise beam-combiners, each output of the combiner receives the equivalent of half of the light from one telescope (the light from N telescopes appear at $2N$ outputs). When observing an object with a H magnitude of 14 then 40 photons are detected during each integration time (assumed to be $2t_0$ at $\lambda = 1.65\mu$m, i.e. 36ms) at each output. The fringe detection scheme is assumed to be one where 2 intensity measurements are made at each output with $\pi/2$ phase steps introduced between them. The two outputs of the beam-combiner are π out of phase so the end result is a set of 4 measurements equally spread across 0 to 2π in phase. Thus there are 20 pixel reads to detect the photons across the 5 spectral channels and 80 photons from the source detected in total.

The sky background level in the H band as measured in La Palma is equivalent to 14.7 magnitudes/arcsec^2. We would expect the higher-altitude MRO site to have no worse sky background, so for a 0.5×0.5 arcsec aperture, we would expect to detect at most 10 photons from the background over the spectral band. In the H-band we expect less than 1 photon per integration from the thermal emissivity of the interferometer optics, assuming 300K optics with a total emissivity of 80%.

The rms fringe contrast degradation for a tip-tilt corrected aperture of diameter $2.4r_0$ is 0.57 and the reduction due to a $2t_0$ integration is 0.79. Combining this with the factor 0.57 reduction due to system imperfections gives an rms fringe contrast reduction of 0.256. The formulae employed for the SNR calculations below use a definition of the fringe visibility V in terms of the normalized Fourier amplitude. For a unit-contrast fringe $V = 0.5$, so the measured value of V is 0.128 when observing an unresolved source.

The ability to track the group delay envelope depends on a monotonic function of a fringe-tracking signal-to-noise ratio defined as

$$\text{SNR}_{\text{track}} = \frac{<V^2> N^2}{N + N_{\text{background}} + n_{\text{pix}}\sigma^2}$$

where $<V^2>$ is the mean squared fringe visibility, N is the number of photons detected from the source per coherent integration, $N_{\text{background}}$ is the number of thermal and sky background photons detected in this time, n_{pix} is the number of pixel reads and σ is the per-pixel read noise. This formula is derived from Buscher 1988 (PhD thesis, University of Cambridge), section 5.1.2 but with the addition of the effects of read and background noise. For the observation of an $H = 14$ unresolved source this SNR has a value of 0.77.

Section 5.1.2 of Buscher 1988 presents simulations of fringe tracking with a 5-spectral-channel group delay system at different SNRs. It was found that fringe tracking could be achieved for values of SNR_track down to 0.33 (N.B. this value has been converted from the "canonical SNR" used in that section). Thus envelope-tracking on a H=14 source should be possible with more than a factor of two margin of safety.

Factors which would reduce this margin of safety include (a) source resolution (b) not meeting throughput and wavefront quality goals and (c) not meeting the detector read noise goal. Factors which could increase the margin of safety include (a) using more advanced fringe-tracking algorithms, particularly those involving detection of linear phase drifts (see Buscher 1988 section 5.1.1) (b) using spatial filtering to increase the fringe SNR (see Keen *et. al.*, MNRAS, 2001) (c) increasing the telescope apertures.

6.6   Tip-tilt sensor

Tango and Twiss (Progress in Optics, 1980) show that differential tilt correction errors with an angular variance of $\sigma^2 = 0.0784(\lambda/D)^2$ will cause a 10% reduction in fringe contrast compared with perfect tip-tilt correction. The uncorrected tilt variance due to the atmosphere is given by $\sigma^2 = 0.680(D/r_0)^{5/3}(\lambda/D)^2$ so in the H band the tip-tilt servo must reduce these tilt aberrations by a factor of 36 over the uncorrected fluctuations. The tilt correction system will suffer from errors from two principal sources: the first is the finite bandwidth of the tilt-correction servo loop and the second is errors due to photon and readout noise in the tilt sensor. We assume that the system is designed to distribute the error equally between these, so that each error source introduces half the allowed variance.

Roddier (1999 Fig. 3.7) shows that the residual tilt can be reduced to 10^{-2} of the total uncorrected atmospheric wavefront variance by a first-order servo loop with 3 dB bandwidth $f_{3\text{dB}}R/v = 0.8$ where R is the telescope radius and v the effective wind velocity, i.e. $f_{3\text{dB}} = 11.4$Hz for $v = 10$m/s and $R = 0.7$m. Now the total uncorrected tilt error is 90% of the total wavefront error so the tilt variance has been reduced by a factor of 90 at this bandwidth, i.e. more than the required amount.

Tango and Twiss (1980) show that, for a photon-noise-limited quad-cell detector the total differential tilt variance due to photon noise is given by

$$\sigma^2 = \frac{2\pi f_{3\text{dB}}}{N_g}\left(\frac{3\pi\lambda}{16 < k > D}\right)^2$$

where N_g is the number of detected photons in the tilt sensor per second and $< k >$ is a factor which takes into account the degradation of the tilt-sensing image quality from that of a diffraction-limited image at the same wavelength. For a visible-wavelength sensor on a 1.4m telescope, i.e. $D/r_0 \approx 10$, Buscher (1988 Fig 5.8) gives a quality reduction factor of about 0.15. However this is in comparison with a visible-wavelength diffraction-limited image, so in comparison to an H-band diffraction limited image, $< k > \approx 0.50$. Optical aberrations in the tip-tilt system may make this 10% worse so we adopt a value of $< k > = 0.45$. With a $V = 16$ source and 30% total efficiency, $N_g = 4170$ photons/sec in the V and B bands combined. Thus the tilt variance due to photon noise is $\sigma^2 = 0.0294(\lambda/D)^2$ which is comfortably inside the required goal of $0.0392(\lambda/D)^2$

7   Array configuration

The layout of the array on the Magdalena Ridge will be largely constrained by the local topography of the site. Fortunately, the site contains a relatively large plateau situated at a saddle point on the mountain. Both the unit telescopes themselves and the beam combination building will need to be accommodated on the site. The essential requirements for the array layout, and possible solutions, are outlined below.

7.1   Requirements

- The array should provide coverage of the uv-plane to allow delivery of the top-level interferometer science requirements. These include minimum and maximum angular resolutions, a capability for "snapshot" imaging, and the ability to provide fully resolved images such that in any individual image a range of angular scales of order 5–10 is present.

- The array configuration should allow phase-bootstrapping so as to permit on-source measurements on long interferometer baselines where the source being studied may have low intrinsic visibility.

- Beams from the unit telescopes delivered to the beam combining laboratory should have the same polarization state and field orientation so as to not reduce the system visibility significantly.

- Beam transport from the telescopes to the beam-combining laboratory should be straightforward, easy to maintain and as inexpensive as is possible without compromising the quality of the beams.

- If at all possible, the beam transport from the telescopes to the beam-combining laboratory should allow for expansion of the array's capabilities in the long-term.

- The array layout must be feasible given the topology of the site, and permit location of a suitably long beam combining laboratory and access facilities for the telescopes and other parts of the mountain top.

- It is desirable that the array be located on a level plane to minimize the amount of longitudinal dispersion that has to be corrected with additional optical elements.

7.2   Meeting the requirements

The solution outlined here assumes an array of 10 telescopes. These will be laid out in an equilateral "Y" configuration with a central telescope, and with three roughly equispaced telescope locations along each arm. A survey of the site has shown that if the unit telescopes are located in a horizontal plane, as is desirable from the point of view of minimizing longitudinal dispersion, then the elevation differences between this virtual plane and the actual ground can be reduced to no more than $\pm 1\,\mathrm{m}$ for a number of layouts.

One highly suitable configuration is depicted schematically in Fig, 1. This is an equilateral Y, with arms pointing along bearings 43° (N arm), 163° (S arm), and 283° (W arm). The site allows the W and S arms to be at least 220 m in length, but the N arm encroaches on the forest at a distance of ∼ 180 m from the center of the Y. Nine of the telescopes are located along the three arms of the array, while the centre telescope is displaced slightly from the center of the Y so as to allow separate optical systems to be located there to support the central beam steering mirrors. The beam combining building itself runs parallel to the W arm, but to the East of the array centre along a bearing of 103°. The site is relatively flat in this direction, though to keep the laboratory level the ground towards the final section of the laboratory will need to excavated by up to 2 m. An alternative location for the beam combining building is along a bearing of 343°, i.e. parallel but north of the southern arm of
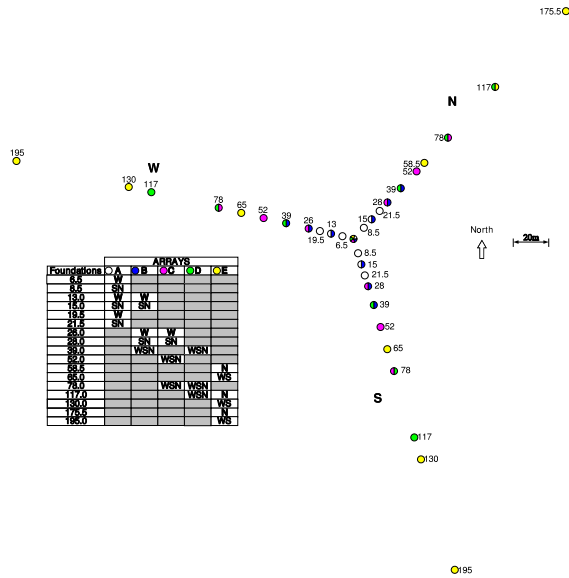
Figure 1: Schematic proposed array layouts for all configurations.

the array. This may offer some advantages from the point of view of wind shadowing, but will need to excavated deep into the surrounding terrain and has some negative impact on possible telescope designs.

In order to satisfy the very large range in angular sizes expected for the interferometric targets, we envisage a total of 5 different array configurations (i.e. akin to the VLA configurations) for the array. The most compact of these, hereafter referred to as the A configuration, would have unit spacings of roughly 6.5 m. This is the smallest spacing that can realistically be allowed given the space envelopes of the ∼ 1.4 m diameter telescopes. A close-up of this compact configuration is shown in figure 3. Three other scaled configurations, B, C and D, would double this unit spacing sequentially from approximately 13 m to 65 m. A final maximum-resolution E configuration, would then use spacings of 65 m on the longer W and S arms, and spacings of 58.5 m on the shorter N arm.

This overall scheme has a useful advantage that expansion from one configuration to the next re-uses many of the foundation pads. Furthermore an increase from 10 to 13 telescopes to the array would not require any additional foundations to be built, save for those required for the longest baseline configuration. Of course, the availability of multiple foundation pads will allow for a great deal of flexibility so that one could envisage "hybrid" configurations involving any user-specified mixture of short and long spacings. Diagrams of the different primary array configurations, together with a hybrid

Name	Nominal spacing	$B_{\min}$	$B_{\max}$	Distance from center
A	6.5 m	6.5 m	37 m	C,W{6.5,13,19.5},S{8.5,15,21.5},N{8.5,15,21.5}
B	13 m	13 m	68 m	C,W{13,26,39},S{15,28,39},N{15,28,39}
C	27 m	26 m	135 m	C,W{26,52,78},S{28,52,78},N{28,52,78}
D	39 m	39 m	203 m	C,W{39,78,117},S{39,78,117},N{39,78,117}
E	65 m	58.5 m	338 m	C,W{65,130,195},S{65,130,195},N{58.5,117,175.5}

Table 2: One possible array configuration for the MRO interferometer. The 10-element equilateral layout, with a shorter East leg, described in the text has been assumed. In this case, the total number of foundations required is $1 + (2 \times 10) + 12 = 33$.
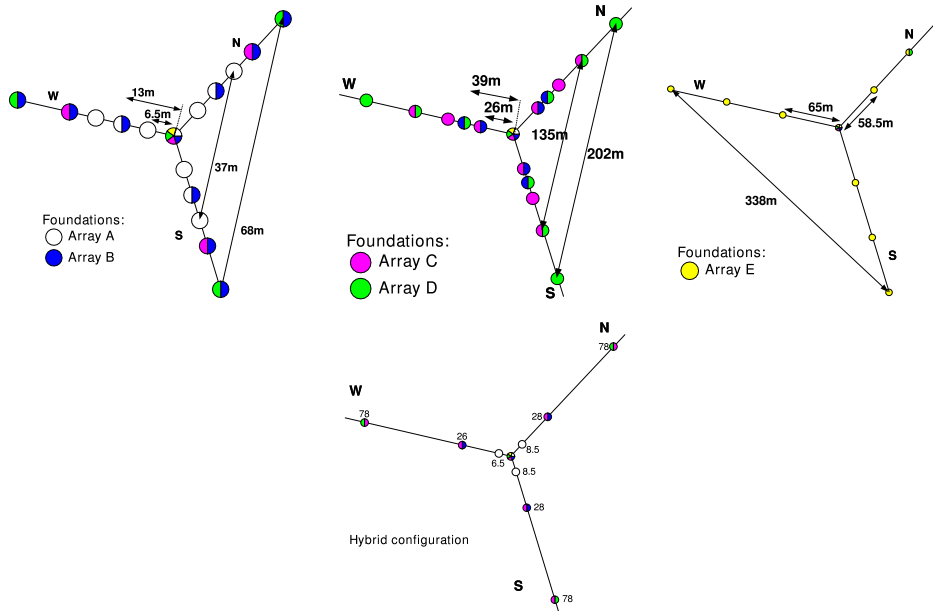
Figure 2: Proposed array configurations, with individual layouts shown in more detail. Note the re-use of different foundation pads as the array is expanded. The lower panel shows an example of one of the many possible "hybrid" arrays, in this case allowing for the detection of both compact and larger scale image structures. North is to the top and East to the right.

configuration, are shown in Fig 2 which also shows them rotated correctly with respect to the cardinal directions.

One final aspect of the overall array layout that deserves mention is its orientation with respect to the cardinal directions. In the context of the local meteorology, the layout of the arms of the array means that there will be relatively little wind shadowing when the prevailing winds are from the south-west or north west. This is the most frequent situation in the summer and winter months. Furthermore, the location of the beam combining laboratory is also favorable in this case. As far as sky coverage is concerned, the proposed array layout will allow excellent coverage to the south and west, with some small obscuration to the east due to the proximity of the forest. It is not expected that this will impact significantly on any of the key science programmes proposed for the facility.

At this moment in time the seismic activity on the site has yet to be investigated. Existing records show that the Magdalena Ridge suffers from moderately frequent but low-level seismic tremors. In-situ measurement of the site is currently planned for fall 2002, and is summarised in more detail in section 5.

Examples of the uv-coverage for the maximum resolution E configuration are shown in Fig. 4. The lower-resolution configurations give almost identical Fourier plane coverage apart from a global scaling factor.

7.3 Budget

Figures appropriate to the development of the site are provided elsewhere in the section on general and interferometer infrastructure. We expect the major costs to be associated with the following three tasks:

1. Grading the site along the arms of the Y, at the location of the beam combination building and where access roads are required.

22
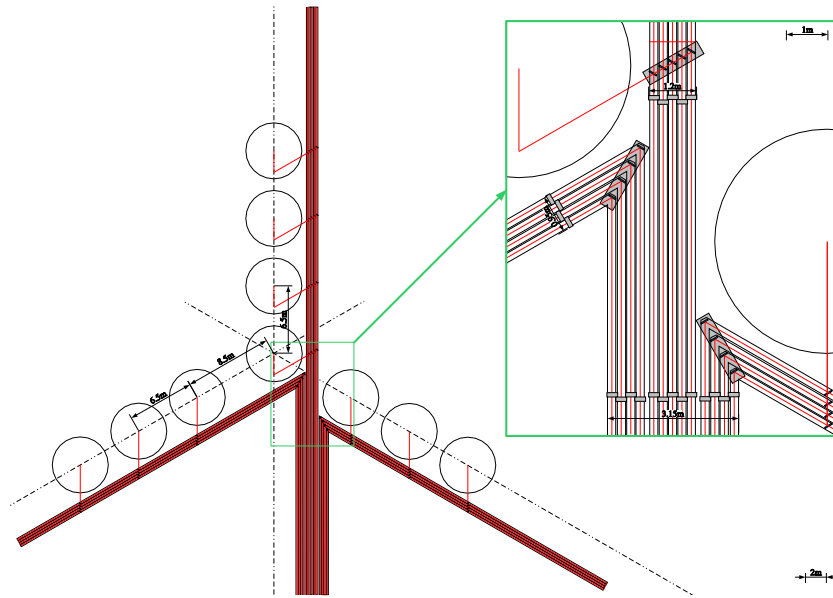
Figure 3: A close-up of the central part of the array when arranged in the most compact configuration. Note how the finite size of the telescope enclosures force slightly uneven spacings between the centre array elements.
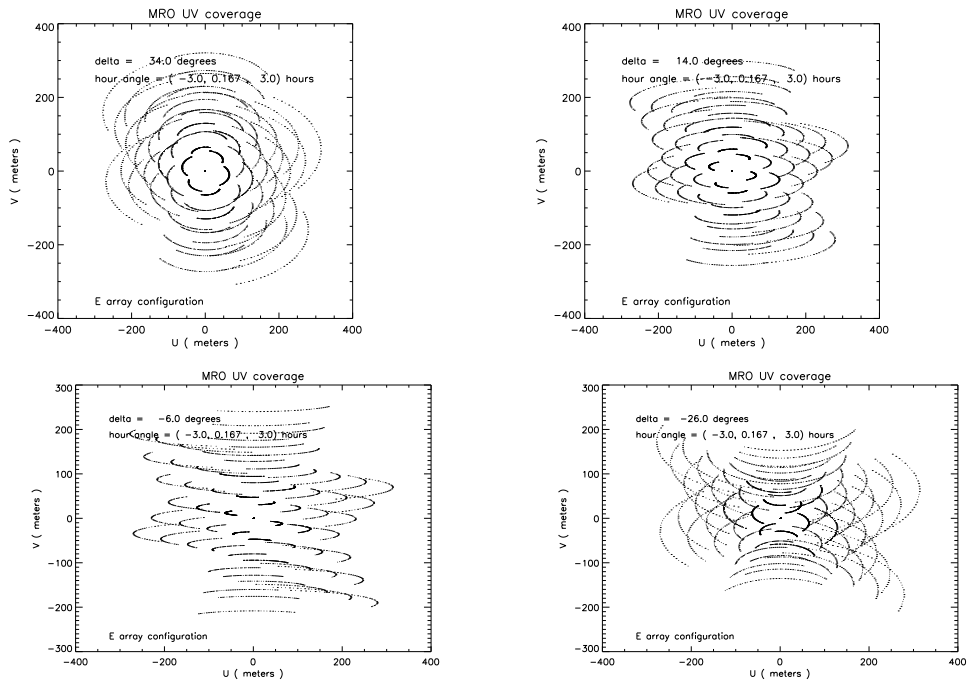
Figure 4: E configuration *uv* coverages for declinations +34°, +14°, −06° and −26°. In all cases a six hour observation has been assumed, leading to excellent coverage of the Fourier plane.

2. Excavating and laying the foundation pads for each telescope location.

3. Laying the telescope access roads along each arm of the interferometer.

8 Unit telescopes - UTs

We explore here the nature of the fundamental array elements, in particular the special requirements related to interferometric performance. Our broad philosophy is to build a usable system with room for growth with the primary endeavour being to do astrophysics.

8.1 Requirements/issues

- The UTs should have a minimum aperture diameter of $1.4\,\mathrm{m}$ to realise the top-level sensitivity goal.

- The UTs should deliver a collimated output of at least $75 \pm 1\,\mathrm{mm}$ diameter to the beam combining laboratory. The direction of this output should be independent of the pointing direction and should be parallel to one of the interferometer arms.

- The output beam should be at a convenient height (e.g. $\sim 1.5 - 2\,\mathrm{m}$ above ground level) for delivery into the beam combining laboratory without additional reflections.

- The optical configuration should allow a collimated beam sent from the beam-combining laboratory to be returned back to its source via a flat.

- The output optical wavefront quality should satisfy the following requirements defined in terms of differing sized zones at the aperture:

Table 3: Wavefront quality error budget. These figures assume an r_0 value of $13\,\mathrm{cm}$ at $500\,\mathrm{nm}$ ($0.75''$ seeing), oversized input beam diameters of $4r_0$, and a maximum allowable rms wavefront error of $\lambda/20$. Note that since the telescope apertures are unlikely to be as large as $1.5\,\mathrm{m}$ in diameter the final three lines of the table can be ignored.

Equivalent input aperture	Wavelength	RMS wavefront error
$66\,\mathrm{cm}$	$0.60\mu\mathrm{m}$	$0.030\mu\mathrm{m}$
$108\,\mathrm{cm}$	$0.90\mu\mathrm{m}$	$0.045\mu\mathrm{m}$
$160\,\mathrm{cm}$	$1.25\mu\mathrm{m}$	$0.062\mu\mathrm{m}$
$223\,\mathrm{cm}$	$1.65\mu\mathrm{m}$	$0.082\mu\mathrm{m}$
$316\,\mathrm{cm}$	$2.20\mu\mathrm{m}$	$0.110\mu\mathrm{m}$

- The field of view over which the above wavefront quality needs to be maintained is $\pm 2''$. The UT optics should give $\sim 0.5''$ image quality over a field of view of $\pm 30''$ for an acquisition/guiding camera at the telescopes.

- The maximum allowed uncorrected wavefront curvature (i.e. defocus) at the output beam (centre-to-edge) should be $90\,\mathrm{nm}$.

- The high frequency optical path stability of the telescopes should introduce no more than a $\lambda/20$ rms fluctuation over a $2t_0$ exposure time as tabulated below:

- The low-frequency optical path stability of the UTs should introduce no more than a few tens of microns of extra OPD over a time of order 6 hours. This should be introduced smoothly, and be repeatable between telescopes and for any individual telescope.

- The design should allow sufficient space to allow pick off mirrors to feed a finder and (possibly separate) autoguider system at the telescopes. There must also be space to allow an atmospheric dispersion corrector (ADC) and a fast guiding mirror to be located in the beam path.

Table 4: Optical path stability error budget. These figures assume a t_0 value of 4.2 ms at 500 nm (0.75″ seeing), and a maximum allowable rms OPD path fluctuation of $\lambda/20$ over an exposure time of $2t_0$.

Exposure time	Wavelength	RMS OPD fluctuation
10 ms	0.60μm	0.030μm
17 ms	0.90μm	0.045μm
25 ms	1.25μm	0.062μm
35 ms	1.65μm	0.082μm
50 ms	2.20μm	0.110μm

- The UTs must operate with high throughput between 0.6μm and 2.4μm.

- There should be only a small differential linear retardation between different telescope outputs. It is not a top-level requirement that the polarization state of the output beams be constant for different pointings, but if this can be achieved so much the better.

- The absolute telescope pointing should be better than 10″ over the whole sky.

- The telescope tracking must be better than 1″ over a timescale of a minute.

- The slewing speed of the UTs should be no slower than 1° per second on the sky.

- The sky coverage of the UTs will be determined by the desire to track sources for approximately ± 3 hours around transit for sources in a range of declinations around $+35°$. It is desirable to be able to operate for all elevations above 30° and to be able to access the pole.

- The UTs and their enclosures need to be relocatable between different foundation pads on the site. The time to reconfigure the whole array of 10 telescopes must be about a week.

- The UTs and their foundations need to be stable at the level of $\sim 100\mu$m over timescales of a month.

- The UTs should be able to operate to specification with wind speeds of up to 9ms^{-1} (20 mph) and in temperatures in the range $-5° < T < 20°$.

- The covers should be able to withstand wind speeds of up to 50ms^{-1} (110 mph) and the ice and snow loading associated with the site in winter.

- It is desirable that the UTs and their enclosures allow inter-telescope separations of as small as 5 m.

- It is desirable that the total power dissipation of the telescopes (including thermal, optical, and seismic outputs) be as low as possible so as not to damage the optical quality of the output beam and environment.

- When not observing, the UT enclosures should provide control for temperature, humidity, dust fraction and light.

In the following section we outline some possible alternatives for the telescope design. Eventually we expect to decide from these based on, for example, total wavefront error, throughput, polarization fidelity etc as well as mechanical feasibility and costs.
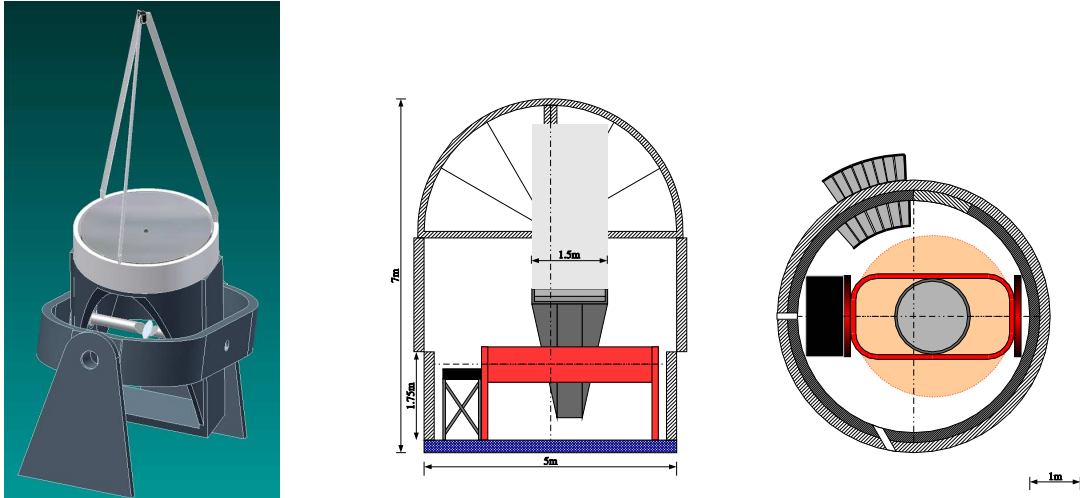
Figure 5: An artist's impression of the Alt-Alt design proposed in this report. In this design the two horizontal axes cross below the surface of the primary mirror where an articulated tertiary mirror intercepts the collimated beam. The image on the left shows an f/2.5 configuration without any enclosure. The images on the right shows an enclosure which attempts to minimise the smallest spacing between telescopes.

8.2 Proposed solutions

One possible solution is to use an Alt-Alt three mirror telescope design (see Fig. 5) where two horizontal and orthogonal axes are arranged in a plane, with an articulated tertiary mirror at their intersection. The optical beam is redirected out along the outer altitude axis by rotating the tertiary mirror at half the inner altitude axis rate. This is a compact and efficient design, using only three mirrors to deliver a collimated beam in a fixed direction.

In this design each UT will have a fast tip-tilt sensor located at the telescope, and this will provide control signals for a fast guiding mirror. This could be the tertiary mirror, but might be another smaller optic. Each telescope will be equipped with a low-cost finder camera, probably a Peltier cooled CCD, and an atmospheric dispersion corrector for the collimated output beam.

Given the requirement that the telescopes deliver their horizontal output beams at a convenient height, we would not intend to elevate the UTs significantly unless this were a requirement based on the topography of the site. It would be desirable to utilise an enclosure that did not involve any moving parts during observations, e.g. a shed with a roll-off roof. This would allow some control of wind loading, and limit vibration during interferometric measurements.

The dome design requires some care as the requirement to have a minimum spacing close to 5m is a difficult one to meet. Figure 5 shows a design which allows a 6.5m minimum spacing.

An alternative design is to use a polarization preserving elevation-elevation mount (Fig. 6). This has six, rather than three, reflective surfaces but has all its reflections with low angles of incidence. This gives a small benefit in terms of polarimetric invariance at the expense of throughput and wavefront quality. On the other hand, the additional optics allow for significant alignment adjustments and the telescope structure is short, thus requiring a small dome and minimizing vulnerability to wind shake.

Both of these mechanical designs can accommodate different optical designs. The two that we have begun to explore are a conventional afocal Cassegrain in which both primary and secondary mirrors are parabolas and a Dall-Kirkham design, in which the primary is ellipsoidal and the secondary is spherical. The Cassegrain delivers a wide field of view but there are challenges associated with keeping the mirrors aligned in the presence of five degrees of freedom. The Dall-Kirkham has a much smaller
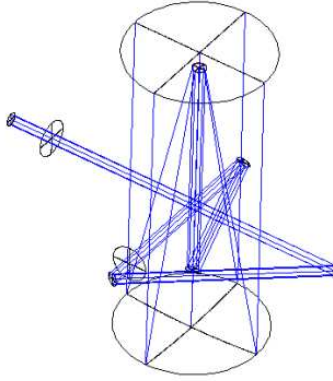
Figure 6: A ray-trace of the polarization-preserving elevation-elevation mount. In this design there are six mirrors, none of which need to be articulated. The principle features of this design are the small angles of incidence off each mirror, which give a moderate improvement in the polarimetric performance of the telescope.

field of view, but the secondary mirror has only three degrees of freedom and so its alignment is more straightforward. At this stage, the second optical configuration appears more promising.

8.3   Budget

At this early stage, the costs of the array unit telescopes are still fluid. To provide some guidance to the reader, we include below the rough costings for one of the designs mentioned above, based on initial discussions with a telescope manufacturer who specialises in professional 1-2.5 m class research telescopes. The readers attention is drawn to both the overall budget and the relative cost of the different subsystems.

Item	Approximate cost/k$
System design/management	255
Optics	5908
Structures	3231
Drive system	3797
Software/control	295
Integration/test	295
Enclosures	1500
Overall total (10 elements)	$15.3M

Table 5: Approximate telescope costings for a 10-element array using the 3-mirror alt-alt telescope design as described in the text. The numbers are based on information provided by a manufacturer who specializes in 1-2.5 m class observatory telescopes.

8.4   Questions for further study

Initial conceptual studies of these telescope designs have already been completed. However, at this stage a number of important additional questions remain:

1. What sort of enclosure design is best and will lead to low induced turbulence?

2. How difficult will it be to achieve the static wavefront quality specifications and then maintain them in the field?

3. How difficult will it be to achieve the dynamic optical path fluctuation specifications, especially in the presence of wind loading?

4. What is the actual trade-off between interferometric S/N and polarimetric fidelity for sources at finite altitudes?

5. What is the specification and design of the ADC?

6. What is the specification and design of the AO system (see later)?

7. How will the telescopes be transported and relocated?

9 Tip-tilt correction

As has been assumed in the earlier section on error budgets, the use of a tip-tilt correction system to correct for the very lower-order wavefront perturbations will be obligatory for realising the top-level astronomical programmes of the array.

It is important to realize from the start that tip-tilt correction alone will be sufficient to meet the sensitivity requirements for the array, provided that reasonable expectations of the seeing are fulfilled.

The issues relevant to how this might be implemented at the MROI are summarised below.

9.1 Requirements/issues

- Errors in the tip-tilt system due to noise or bandwidth limitations should not reduce the rms observed visibility by more than 10 percent.

- The tip-tilt system should not introduce additional piston fluctuations into the beam fed to the beam combining laboratory over and above those arising from the atmospheric refractive index fluctuations.

- It is highly desirable, from the point of view of complexity, that the tip-tilt system use an on-axis source (i.e. the observing target) for sensing the wavefront.

- Numerical analysis by Bharmal (2002, in preparation) shows that it is possible to measure defocus and astigmatism in addition to tip and tilt using the same detector assembly as that needed for tip-tilt sensing. This is not relevant to the design of the tip-tilt correcting system per-se, but may have a bearing on the location of any additional adaptive optics sub-systems.

9.2 Proposed solution

Because of the potentially very long paths back to the beam combining laboratory, it is advantageous to locate the tip-tilt sensor and correcting element close to each telescope. This can be accomplished by picking off light from the target using, for example, a beam-splitter or dichroic plate, focusing the light to a spot with a lens or curved mirror and sensing the spot position using conventional array detectors read out as quad- or 9×9-cell sensors. In the three-mirror telescope design, the tertiary mirror would probably be used for the active correction. In the six-mirror design, we expect that one of M3–M6 will be suitable for this purpose.

To allow adequate tip-tilt correction both for small apertures (used when operating primarily at optical wavelengths) and large apertures (used on the faintest sources) the tip-tilt system will have a variable correction bandwidth, from a few Hz to approximately 50Hz. This implies a sampling bandwidth of 500Hz or more, which should be easy to achieve with modern CCD detectors readout in limited-format modes.

A slow ($\sim$ 1Hz bandwidth) and separate tip-tilt system may be needed to remove instrumental beam drifts occurring downstream of the telescopes within the beam pipes, delay lines and beam combining laboratory. This could use light from the source or alternatively use an artificial reference source propagated out from the beam combination laboratory.

9.3 Questions for further study

At this stage a number of questions need further thought. These include:

1. What wavelengths should the tip-tilt sensor operate at? An initial study in Cambridge suggests that a single optical sensor working from 0.4μm to 1.0μm might be suitable for all targets of interest. As long as the total throughput to the sensor can be maintained at 30% or higher in the

B and V bands, sources with V magnitudes brighter than 16 should be tracked satisfactorily. A more thorough analysis is currently underway to investigate whether or not this will cope with all possible science programmes

2. Is a slow tip-tilt system really needed if the path compensation trolleys employ cat's-eyes rather than roof mirrors?

10 Adaptive optics

One of the strategic aims for the MROI will be to investigate the potential of adaptive correction beyond tip-tilt for optical and near-infrared interferometry.

There is currently no direct link from the astronomical programme for the array to the adaptive optics (AO) requirements. Instead, we expect to explore the combination of interferometry with AO as a technical programme in parallel with the main astronomical aims of the array. As a result the requirements and specifications for this subsystem are not as well developed as for the rest of the array. The following subsections therefore indicate the issues that need to be explored and routes to reaching a decision on these in a timely fashion.

It seems likely that the resources required to implement AO at the required level on all the telescopes will be larger than the resources available in the currently agreed funding profile. Therefore it is necessary to look at a staged design: in "Stage 1", which is encompassed within the existing funding profile, demonstrations of the basic technologies for combining AO with interferometry are performed; in "Stage 2" it is assumed that further funds become available and AO is deployed to maximum effect on all the telescopes of the array.

10.1 Requirements/issues

1. What role should AO play in Stage 2?

   (a) Increased SNR/data rate on brighter sources? On sources of sufficient brightness to drive a high-order wavefront sensor the addition of an AO system would allow larger apertures to be used. This could provide a useful improvement of the fringe SNR for in very narrow bandwidths or heavily resolved sources, but this must be compared with the improvements offered by doing phase-referenced averaging with smaller apertures.

   (b) Better data accuracy in poor/varying seeing? An AO system with a large number of actuators per r_0 and a sufficiently bright reference source to drive the wavefront sensor at high SNR offers the possibility of improving the wavefront quality to a sufficient extent that the fringe contrast is not substantially affected by changes in the seeing. This would improve calibration accuracy, but this must be compared with the improvement in calibration accuracy (at the expense of loss of light) offered by using spatial filters.

   (c) Access to fainter sources? It is possible that an optimised AO system could work on sources up to one magnitude fainter than the fringe-tracking limit of a tip-tilt-corrected interferometer. In such a case the improvement in wavefront quality from the AO system might be sufficient to allow fringe tracking on these fainter sources.

2. Which of the above aspects do we need to test in Stage 1?

3. What wavelength is correction to be optimised at?

4. How does the adding of an AO capability interact with the rest of the interferometer?

10.2 Proposed solution

The above questions need to be addressed in a systematic way. The proposed plan of development is as follows:

1. Address, through simplified analytical and numerical studies the question of what numerical gains in criteria 1(a)-(c) above are to be had from an idealised AO system of radial order N at wavelength λ for a telescope size D, seeing r_0 and t_0 and wavefront sensor photon rate P per r_0^2 per t_0. Derive typical values for a set of assumed MRO parameters.

2. In parallel, make a list of top priority science goals and see which of 1(a)-(c) is most important. This would be done by examining each science goal in turn and asking how much of a difference 1(a)-(c) would make in achieving that goal.

3. Decide on the basis of the results of steps [1] and [2] what technical goals are desirable in principle in order to achieve the MRO science goals as well as possible.

4. Decide which scientifically useful subset of these technical goals are achievable in Stage 1 and which are achievable in Stage 2.

5. If there are goals which are both desirable and achievable in Stage 2 but are not achievable in Stage 1, decide which technical goals are most important to address so that we are ready for Stage 2 funding.

6. Decide on which AO solutions meet the criteria decided on in steps [4] and [5].

7. Decide placement of the AO system within the interferometer.

8. Narrow down AO subsystem design to one or two concepts.

9. Initiate (parallel) design studies on these concepts with the aim of

   - Determining how well they meet the goals decided in [4] and [5]
   - Arriving at an overall estimate of budget to completion.

10. Decide on AO system concept based on the result of design studies in stage [9] and the resources available from overall interferometer budget. Proceed with full design/build.

Step 7 above, a decision on where the AO system is placed in the interferometer beam train, is in the critical path for the rest of the interferometer design. Two possible positions for the AO system are:

On a fixed platform in the telescope enclosure. The AO system would be on a removable kinematic mount as illustrated in figure 7. High interferometric throughput designs (i.e. ones with small numbers of surfaces between the telescope and the interferometric beam combiner) would be possible because the beam is already very close to a conjugate with the telescope pupil when it enters the AO system. High wavefront sensor throughput is possible because there are only a few surfaces from the telescope to the entry port of the AO system.
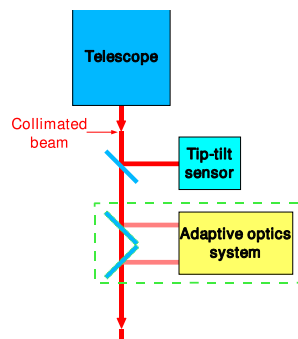

Figure 7: Diagram illustrating the concept of a modular and removable AO system. In this design the AO system picks off the collimated beam after the standard tip-tilt sensor and returns it as a collimated beam to the beam combining laboratory. The system is removable so that the undisturbed beam can be accessed rapidly if the AO system is not required.

33

In the beam combining laboratory. This would once again be a removable AO system but the placement in the laboratory offers a more thermally stable environment and one where it would be possible in principle to switch a small number of AO systems between a large number of beams on timescales of order of minutes. The entrance to the AO system would be a long way from conjugate with the telescope pupil if only flat mirrors were used in the beam train. This lack of conjugation is a concern for reasons not primarily to do with field of view (the interferometric field of view is very small anyway and it is assumed that on-axis reference sources would be used) but rather to do with scintillation: the long propagation distances mean that wavefront perturbations in the beam on the scale of the Fresnel zone size (for propagation over a distance of 200m, the Fresnel zone size is 14mm at a wavelength of 1 micron) would be converted from phase perturbations into amplitude perturbations, which cannot be corrected with a deformable mirror. Thus some means of restoring pupil conjugation are needed, and some ideas on this are outlined in the beam relay section.

The placement of the AO system has an impact on the design of the rest of the interferometer and should therefore be decided as early in the design process as possible. This decision should take account of the desire to optimise the operation of the interferometer both in tip-tilt-only mode and in any modes where the AO system is being used.

10.3   Timeline and budget

Steps [1] and [2] above could be started immediately, with the aim of having written reports of the results by mid-December 2002. A decision on [3-8] could be made in December 2002 and design studies [9] would be started at this time. The decision on the final AO system concept in stage [10] would be made by March 2003.

Resources up to and including step 8 could be mostly met from internal MRO Project Office and Cambridge resources (Loos, Teare, Horton, Buscher, Haniff, Bharmal) but could also involve resources external to the Project Office but within the MROC (Voelz, Chang). The budget for stage [9] is extremely unclear but a ball-park estimate is $20k each for the initial design studies and somewhere in the (large) interval $0.2M-$2M for design/build in stage [10].

Task	Dates	Effort
1 - Quantify gains that AO delivers	Now - Dec 02	In house
2 - Assess impact of gains on top level science	Now - Dec 02	In house
3 - Agree on technical goals needed to deliver top-level science	Dec 02	In house
4 - Agree on feasibility of investigating these	Dec 02	In house
5 - Agree on priorities for Stage 1 and Stage 2 development	Dec 02	In house
6 - Decide what type of AO system is thus required	Dec 02	In house
7 - Decide on placement of AO system	Dec 02	In house
8 - Narrow down AO system to one or two concepts	Dec 02	In house
9 - Initiate design studies for these concepts	Dec 2002 - Mar 2003	TBD
10 - Identify preferred system and initiate build	Mar 03	TBD

Table 6: Summary of approximate timeline for the AO development strategy described above.

11 Beam transport

Since the UTs will be located some distance from the beam-combining laboratory a scheme for delivering the beams in an efficient manner is required. This will necessitate considering at least the following issues:

11.1 Requirements/issues

- The transport system must deliver light over the full bandpass required for the top-level science goals at all times.

- The field-of-view transmitted by the transport system must at least meet the requirement imposed by the top-level science case, i.e. the width of the unit telescope primary beam (0.5 arcsec at K band). A larger field of ± 1 arcsecond should probably be allowed for in the design.

- The transport system should introduce minimal spatial and temporal aberrations to the stellar wavefronts.

- The transport system should be as efficient in terms of throughput as possible.

- Visibility losses due to diffraction, polarization and longitudinal dispersion should be kept to a minimum.

- The transport system must be able to cope with array reconfiguration and allow easy access to all elements of the array for maintenance purposes.

- In addition to the requirement on visibility losses, we must consider the impact of the beam transport system on the polarization state of the beams.

- The additional requirements that would be imposed by locating the adaptive optics systems in the beam-combining laboratory must be investigated.

11.2 Simplest solution

The simplest solution is as follows. We would use metal pipes containing low-pressure air for beam transport. Each transport pipe will have two flat anti-reflection coated windows, and will use only two internal mirrors to direct the beam to the beam-combining laboratory (see Fig. 8). This scheme uses a symmetric arrangement of parallel mirrors and introduces no differential polarization changes between beams. The angles of incidence on the two mirrors are 30 degrees, and so the beam transport system does not significantly change the polarization state of the beam supplied by the telescope.

An air pressure of 0.01 bar will reduce the internal dispersion to just 1% of that of the equivalent air path, i.e. smaller than that at COAST where no dispersion correction is employed. Oil-free vacuum pumps are available to deal with this type of volume/pressure, and should be used so as to eliminate the chance of contamination of mirror coatings. A beam width of 75 mm is adequate to minimise diffraction losses for tip-tilt corrected beams for paths at long as several hundred metres at optical and near-infrared wavelengths. This implies pipes with an internal diameter of perhaps twice this size.

The vacuum pipes will be joined with rubber sleeving, as in CHARA and NPOI (or metal bellows as at SUSI), and will be supported at the height that the beam exits each telescope (i.e. at the height of the tertiary in the three-mirror telescope design). The supports for the beam-directing mirrors will need to be separate and isolated from the supports for the pipe itself. Shutters will be located at strategic locations so that work on the beam-directing mirrors will be possible without opening up the whole system to atmospheric pressure.

With as many as 10 telescopes the physical layout of the pipes is important. The scheme depicted in Fig. 8 shows how each telescope location can feed any of the beam pipes in its arm of the array Y.
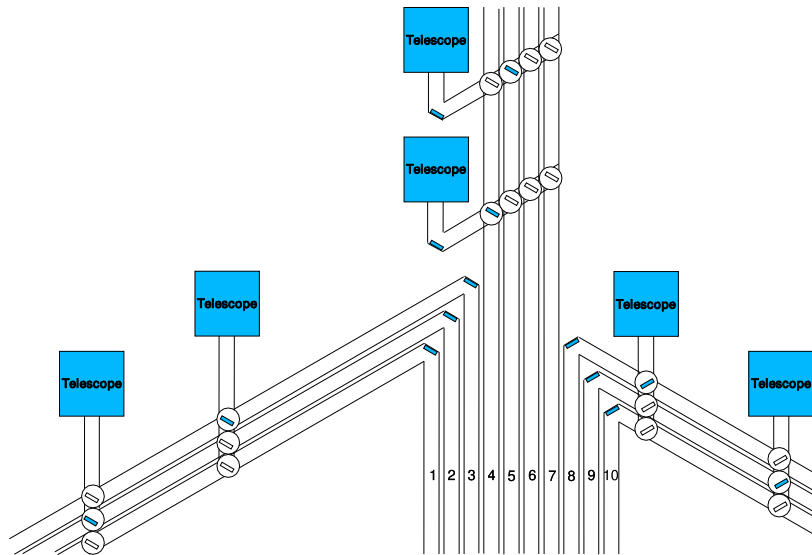
Figure 8: Proposed pipe layout for a 10 telescope Y array. Note how only 2 reflections are required to feed the beams from each telescope to the beam combining laboratory. Each telescope can send its output down any of the beam-pipes along its arm of the Y.

This is an important feature giving flexibility when re-configuring the array, and in situations when a telescope may have failed and be temporarily out of use.

11.3   Alternative designs

We have also considered a beam relay system where the beam from each telescope is directed *outwards* along the relevant arm before being reflected back into the beam combining building. The arrangement of mirrors and vacuum pipes (the equivalent of Fig. 8) has not been decided for this option, but it is clear that the fold mirrors would have to be moved whenever the array is reconfigured.

This folded beam transport system reduces the required length of the delay lines, and hence the beam-combining building, from 186m to 150m (see delay line section). This is achieved at the cost of one extra reflection per beam plus extra vacuum pipe-work and associated supports outside the building. Larger pipe diameters will also be needed.

The main advantage of this layout is realised by changing from an afocal system to one in which the beams are brought to a focus in a plane near the entrance to the building (this could be a temporary change). The beams have all travelled the same distance from the telescopes, and so are all conjugate to the same height in the atmosphere (refer to the AO section). We can thus envisage adaptive optics systems that are interchangeable between beams. This would permit a small number of systems (three or four?) to be shared between ten unit telescopes, although the imaging capability of the array would be severely compromised by only measuring a few baselines and closure triangles at once.

A further development of this system would involve full pupil-relay to the AO system location, using field lenses. The trade-offs between more complicated relay systems and possibly improved AO performance need to be investigated.

11.4   Budget

To give an idea of the approximate budget for the beam transport systems, we provide below (Table 7) estimates for the simplest possible relay train outlined above. We include only hardware costs at this

Item and cost breakdown	Total cost/k$
1500 m of 15cm dia vacuum pipe @ $40/m	60
Assuming 4m pipe lengths: supports and 400 joints @ $500 each	200
Optical windows for pipes - 1 per foundation + 10 @ $1000 each	43
Mirrors - 3 per foundation @ $500 each	50
Mirror mounts - 3 per foundation @ $1000 each	99
Vacuum pumps, gauges and sensors	40
Overall total	$0.49M

Table 7: Approximate costings for the simplest possible beam transport solution. A total number of 33 telescopes foundations has been assumed.

stage. Clearly, these data only give an indication of price for one option, but they are useful nonetheless in assessing how the relative costs of different options might scale.

11.5 Questions for further study

Although vacuum systems have been used successfully in a number of interferometric arrays for many years, e.g. the Mark 3, NPOI and SUSI, the large number of telescopes proposed for the MROI and its potentially difficult site mean that at least the following questions remain unresolved:

1. Would a single large pipe along each arm be a better solution?

2. Do we want separate vacuum systems for each arm/telescope?

3. What sort of environmental protection is required/desirable for the transport pipes?

4. What are the safety implications in the case of a rupture of the transport pipe system?

5. How do we accommodate thermal expansion and how are the pipes isolated from the telescopes and beam combining laboratory?

6. With all the pipes in place, how will this impact on moving around the site and relocating telescopes?

7. The more complicated beam transport options need to be evaluated in the context of decisions about the number and type of AO systems to be procured.

12   Delay Lines

The delay lines are a critical subsystem in the array. The relevant issues to be considered include:

12.1   Requirements/issues

• We need to match paths from a star, via a pair of telescopes, to within the coherence length of the light being measured in any spectral channel of the detector system.

• The delay line system must be able to introduce a given absolute delay with a precision significantly better than the random perturbations introduced by the atmosphere, i.e. of order a few microns.

• The delay line carriages must respond to path-correction signals from the fringe acquisition and tracking signals in real time. Latencies of less than a millisecond for small amplitude signals are desirable if phase tracking is to be implemented.

• The maximum slew-rate of the delay line carriages should be commensurate to the slewing time of the unit telescopes. This corresponds to a rate of $\sim 0.5\,\mathrm{m\,s^{-1}}$.

• Given an accurate position of the telescopes, local Sidereal time, and a star position, the delay line carriages must track fringes for long periods. The fringe jitter introduced must be less than $\lambda/40$ during an exposure time as defined by Table 4.

• For testing purposes it should be possible to introduce a periodic delay modulation similar to that used on the COAST system, i.e. with an amplitude of a few tens of microns at a few Hz. In normal operation delay modulation may be provided separately by subsystems of each beam combiner.

12.2   Proposed solutions

One solution is to use a design based on the COAST design but modified for longer paths. This uses a single stage optical system, unlike the multi-stage systems of CHARA and NPOI to save on reflections. The design consists of a roof mirror mounted on a motorised trolley in a long pipe (see figure 9). The pipe is evacuated to better than 10^{-3} atmospheres to minimise the effects of atmospheric dispersion and turbulence.

This design uses a laser interferometer to measure the position of the roof mirrors: a position and velocity servo running at 5kHz using 1/128th wave HeNe laser fringes can easily stabilise the
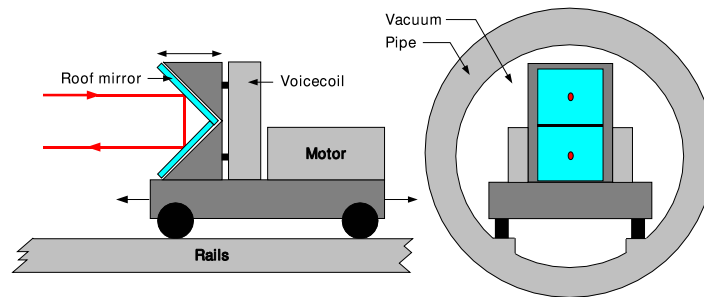

Figure 9: A path compensation trolley with two-stage servo, running on extruded rails in a vacuum pipe. The trolley must be able to deal with beams of diameter at least 75 mm.
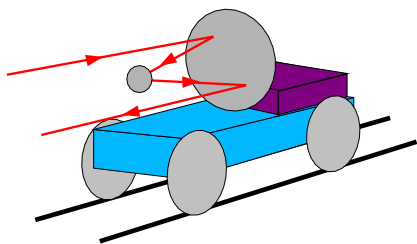
Figure 10: An alternative path compensation trolley design using a cat's-eye retro-reflector instead of a roof mirror. In this scheme the position and tilt of the secondary cats-eye mirror with respect to the focusing parabola must be maintained very precisely.

roof mirror position to the required accuracy. Commercial laser interferometers will work over these distances if a beam expander is used to reduce the effects of diffraction, the system simply counting laser fringes from a reference micro switch.

In the simplest configuration, the delay-line pipes are bore-sited along the directions of the incoming beams from the array so as to avoid extra reflections. A pipe length of 200m allows for delay compensation for any star above the horizon (assuming an equilateral Y array with 200m arms). If need be, a reduction of this requirement to compensation for stars within 60° from the zenith reduces the required pipe length to 186m. A further reduction of this length to 150m can be achieved by adding fixed delays to the path from each telescope such that the internal delays are exactly compensated for a star at the zenith. However, this latter modification would involve adding extra reflections and extra pipe-work and so is not at first sight attractive. This is discussed in more detail in section 11.

This design of delay line carriage requires the roof mirror to remain in the same orientation to within 0.5 arcseconds in azimuth and at the same height to within 1mm as it moves along the pipe. Our plan to achieve this is to have the carriage run on extruded rails (or rails bonded to extrusions in the pipe) and to initially align the pipes along a fiducial to within 1mm when they are installed. The azimuth of the roof mirror must then also be actively controlled either using feedback from a real-time tilt-measuring system or using a look-up table measured at the beginning of the night. In the former case, the tilt-servo can use either starlight or a reference beam from a laboratory source.

An alternative to the roof-mirror design is a cats-eye arrangement, as exemplified by the JPL delay lines (see Fig. 10) in use at Keck, CHARA and NPOI. This arrangement, of a parabola with a flat at its focus, reduces the angular alignment tolerances on the carriage and has less effect on the polarisation state of the incoming beams. Its disadvantages in comparison to the roof-mirror design include the possibility of increased wavefront error due to misalignment of the curved optical element, the fact that the retroreflector assembly will be larger and potentially more difficult to make light and rigid, and the effects of scattering of the metrology light off the secondary mirror.

12.3   Budget

Summary costings and estimated staff effort required for the delay-line system are provided below.

12.3.1   Equipment

12.3.2   Staff costs

12.4   Questions for further study

1. How smooth are rails extruded into aluminium pipe? How fast does any active control of the roof mirror azimuth need to be?

Item and cost breakdown	Total cost/k$
10×200m of 40cm dia pipe 1cm thick @ $500/m	1000
Assuming 4m pipe lengths: supports and 500 vacuum sleeves @ $1000 each	500
Zygo interferometer: 2 laser heads, 10 measurement heads,	
1 VME interface, extra optics, mounts, beam expanders	150
10 optical windows for pipes @ $5000 each	50
Trolleys, computers and mirror parts @ $25000 per trolley	250
Overall total	$1.95M

Table 8: Approximate costings for the delay line system at MROI. A 10 telescope array has been assumed.

Effort and labor type	Total effort
Mechanical engineering design & prototyping	24 man months
Technicians for prototyping	12 man months
Technicians for trolley assembly	30 man months
Alignment of delay line pipes	4 man months
Software design and prototyping	24 man months
Overall total	7.8 man years

Table 9: Approximate staff effort required for the delay line system at MROI. A 10 telescope array, with 10 delay lines, has been assumed.

2. How do we align the pipes to the required precision? Will it be possible to align the pipes when air-filled and maintain the alignment under vacuum?

3. Will bumps in the track at the rail joins be a problem ?

13 Beam combination

13.1 The overall beam combination room

13.1.1 Requirements/issues

The top-level requirements for the beam-combining subsystems in the array can basically summarised as follows:

- There must be a facility to measure interference fringes on a substantial fraction of the 45 baselines and 36 independent closure triangles possible from a 10-telescope array.

- There must be a facility to find the zero-OPD (optical path delay) position for stellar fringes and measure the OPD variations due to the atmosphere. This must work for sources which are as faint as $H = 14$ and for resolved sources which are 5×5 pixels across.

- There must be facilities to assist in the alignment of the whole optical train of the interferometer.

13.1.2 Overall concept

One possible concept that we are considering for the beam combining laboratory is sketched schematically in Figure 11 which shows a block diagram of the major subsystems in the main beam combination
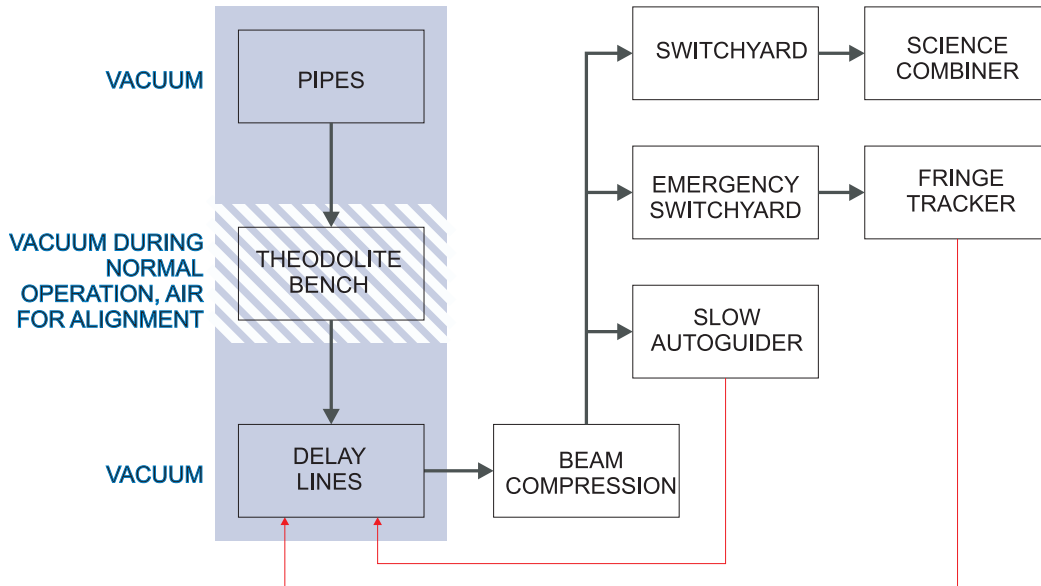
Figure 11: Block diagram of a possible optical train in the beam combining laboratory, including the two sets of beam combiners.

room.

Light from the telescopes exits the delay lines onto a set of optical benches which contain the various subsystems. The beams are initially compressed in diameter, their angle of arrival sensed, and then passed via dichroic splitters into separate fringe-tracking and science beam combiners. Separate combiners are required because the fringe-tracking and science beam combiners must be optimised for conflicting goals:

- The science combiner must combine large numbers of beams to get closure phases and sample as many baselines as possible, while it is more efficient to use pairwise combiners for fringe tracking.

- The science combiner must have low crosstalk between baselines and low calibration errors, while in the fringe tracker it is the raw SNR which is the main important parameter.

- The dispersion of the science combiner is set by science requirements and can be very high, which imposes an unacceptable SNR penalty on fringe tracking.

- For resolved sources it will be valuable to do "wavelength bootstrapping" by using a long wavelength for fringe tracking and a short wavelength for science observations.

It is relatively straightforward to design dichroics that allow for any photometric band to pass to the science beam combiner, while redirecting the other bands, not used by the tip-tilt and AO sensors, to the fringe tracking subsystem. Only a small number of these is required to accommodate the range of choices that might be made in practice. Note that in this scheme, beam compressors are used to allow relatively small beam combining optics to be utilised so that good thermal and mechanical stability can be maintained with little active control.

Depending on the design and specification of the delay lines, it may be necessary to have a slow autoguider to correct tilt drifts in the optical train downstream of the fast tip-tilt system on timescales of a few seconds. This could use a small fraction of the starlight. However, an alternative might be to use an artificial light source, perhaps propagating in the reverse direction to the starlight and sensed at the telescope.

Whatever beam combining scheme is adopted, it is desirable that the vacuum system connecting the beam transport system to the delay lines be demountable to allow system alignment during system commissioning. The beam transport and delay lines would then be separate vacuum systems with windows in place of the connecting pipe. During normal operation there would be a single vacuum system from the telescopes through the delay lines to the beam combination table.

13.1.3 Questions for further study

1. What is the ideal split of light between fringe tracker, science combiners and tip-tilt tracking? This is currently being investigated in Cambridge. Our initial studies show that not only can suitable dichroics be designed, but also that only a small number of these will be required for any science observation.

2. Can suitable dichroic or other beamsplitters be constructed which are efficient and do not introduce excessive phase variations with wavelength? As mentioned above, designs for these beam splitters have already been investigated successfully in Cambridge.

13.2 Beam compressor

13.2.1 Requirements/issues

- The beam compressor must reduce the diameter of the beam to a size where the beam combination optics are manageable in terms of space envelope, path-modulation requirements and maintenance of internal path-length tolerances.

- If the compressed beam size is too small, the effects of diffraction and residual tilts may cause excessive beam broadening or beam shear along the path downstream of the compressor.

- The beam compressor should not introduce an unacceptable level of wavefront error or light loss.
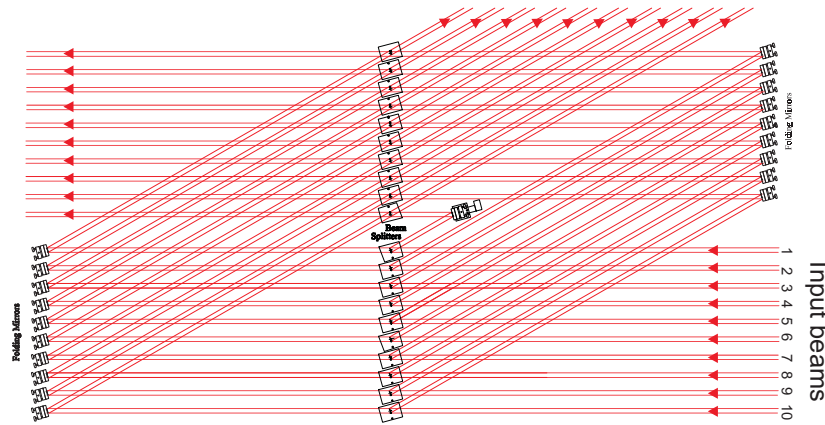
Figure 12: Schematic of a set of pairwise beam combiners for fringe tracking on 7 telescopes (based on the design of ten Brummelaar *et. al.* 2000). The beams enter at the bottom right hand side and exit as pairs of complementary outputs towards the top right and left, having been combined in a set of beam-splitters. In practice, with a reduced beam diameter, this type of combiner could be made out of rigid bulk optics components.

13.2.2 Proposed solution

A compressed beam diameter of 5 mm is compatible with the current compact 4-way beam combiner prototypes that we have built and tested in Cambridge (see Fig. 13), and 7.5 mm beam diameters should be compatible with slightly larger optics. For a 5 mm beam, the Rayleigh distance where diffraction effects become important is 11.4 m for a 2.2μm wavelength and 41 m for a 600 nm wavelength.

Examples of beam compressors that would satisfy our requirements include the off-axis Cassegrain telescope used in the GI2T or those used at NPOI. Other possibilities include a low-f-number system of spherical mirrors which have may have less critical alignment tolerances.

13.2.3 Questions for further study

1. Paths inside the beam combiner may be more than 10 percent of the Rayleigh distance. Does this cause unacceptable losses?

2. Can a system be built which meets a very tight ($\lambda/60$) wavefront spec under alignment drifts etc?

13.3 Fringe tracking beam combiner

13.3.1 Requirements/issues

- The tracker beam combiner must be able to find and track fringes on sources as faint as $H = 14$.

- It must be able to track sources on sources no more than 2 magnitudes brighter than this which are resolved into 5×5 filled pixels.

13.3.2 Proposed solution

A pairwise fringe combiner which combines light from the nearest-neighbour telescopes can be used to phase the array. The exception is for the telescopes at the centre of the array, where a 3-way combiner is needed. Figure 12 shows that the layout for the pairwise combiners can be quite simple.

The three-way combiner would perhaps be based on the NPOI 3-way design or on the COAST 4-way design with one input missing.

To allow for group delay fringe tracking, each output must be spectrally dispersed into a number of bands. Simulations show that 5 channels is adequate, but the optimum number of channels to use will depend on the detector read noise that can be realised.

For faint sources the tracker would operate in envelope-tracking mode, but we envisage this could be switched dynamically in software to run in phase-tracking mode if there were enough light.

13.3.3 Questions for further study

1. What is the optimum number of spectral channels for a group delay tracker?

2. What problems does fitting in the 3-way combiner cause?

3. Would an image-plane combiner offer any advantages?

4. Would the same design of combiner as used for the science combiner be useful for fringe tracking?

13.4 Science beam combiners

Here, the requirements for the beam combining subsystem are as follows:

13.4.1 Requirements/issues

- The combiners must measure the visibility on a significant fraction of the 45 baselines and 36 closure phases sampled by the array.

- They must allow measurement in the R, I, J, H & K bands, although not necessarily at the same time.

- Default spectral resolutions of around 50 should be available.

- Higher spectral resolution over smaller bands (e.g. across H-α) is necessary for certain science projects.

- It must be possible to calibrate fringe amplitudes to at least 1% on bright sources.

- Fringe power crosstalk should be minimized.

13.4.2 Proposed solution

A number of possible beam combination methods are possible. The simplest conceptually is a 10-way all-in-one combiner. An easier-to-implement alternative is to use smaller-way combiners in parallel and then have a beam switch-yard which is capable of switching beams between combiners on timescales of a few seconds to allow all possible combinations to be made.

Possibilities for the science beam combiner include using three 4-way combiners (see Fig. 13) working in parallel or an 10-way combiner shown in Fig. 14. The former combiners have already been fabricated in Cambridge, while the latter have already been designed.

Spatial filtering, either before or after beam combination would allow high-precision visibility calibration, while fast shutters in each input beam would allow rapid calibration of the coupling efficiency into the spatial filters. Spectral dispersion would be provided by exchangeable zero-deviation grisms, with an option for exchanging these for filters in special cases.

Finally, extra mirrors will need to be introduced into the optical path to match the zero-OPD positions in the science combiners with those in the fringe tracking combiner and to allow for modulation in the optical paths of each beam combining assembly.
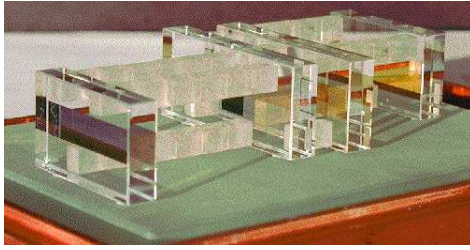
Figure 13: A third-generation COAST miniature 4-way beamcombiner. The total footprint is approximately 20×7.5 cm. This type of bulk optics combiner requires no alignment after fabrication as all the elements are optically contacted and form a solid whole.

13.4.3   Questions for further study

1. What fraction of the available baselines and closure phases must be measured for acceptable imaging performance? This is currently under investigation in Cambridge.

2. What level of crosstalk performance can be achieved with pupil plane combiners? What level is necessary?

3. Image-plane versions of these beam combiners are attractive from the point of view of crosstalk, but require optics which are anamorphic at the 100:1 level. Is it possible to make such combiners with sufficiently low wavefront distortion and high throughput to make them preferable to pupil plane combiners?

10–telescope beam combiner

Shifts ↑ and ↟

25/45 baselines	+ 20/45 baselines
20/120 cl. phases	+ 20/120 cl.phases

9 10 1 2   5 6 1 2
7 8 9 10   9 10 5 6
5 6 7 8   3 4 9 10
3 4 5 6   7 8 3 4
1 2 3 4   1 2 7 8

1
3
5
7
9
2
4
6
8
10

Figure 14: Schematic of a 10-way beam-combiner. The collimated beams enter at bottom left and are combined in quadruples, leaving the combiner at top left and right. This type of combiner can be straightforwardly extended to 12 input beams, with little additional complexity. Movement of only a few components — three in this example — is required to measure all the baselines in the array.

14 Detectors

Various subsystems are critically dependent on detector performance and so here we collate all the relevant requirements and look at common technologies for meeting these requirements

14.1 Requirements

1. 10 tip-tilt sensors each at least 2×2 pixels but perhaps 2 blocks of 3×3 pixels to allow measurement of defocus and astigmatism. Use of B and V wavelengths is preferred so as not to divert light from science bands. High quantum efficiency and low read noise are essential. Minimum frame rate 100Hz, up to 10kHz can be used if photon counting.

2. Visible science detectors: Need to detect in R and I band light from 8-12 outputs of the science beam combiners. Each output has a minimum of 100 spectral channels (but 256 are preferred) and is sampled at up to 10kHz. Detector is to be photon-counting in faint-source mode. High quantum efficiency (typically $> 50\%$ in the relevant wavelength bands), good linearity, dark counts < 10/pixel/second, and dynamic range of $\sim 500 : 1$ are also required.
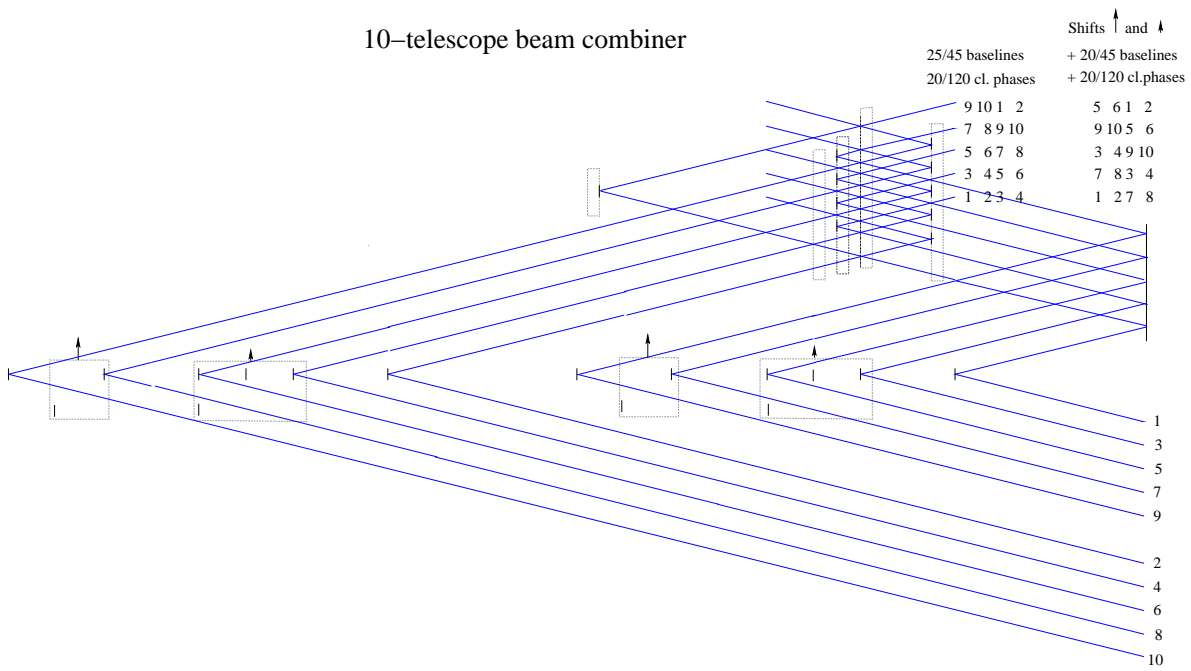
3. 10 finder cameras (16th magnitude sensitivity at R with 1.4m telescope). 1 Hz frame rate required and up to 10 seconds integration for faint sources. Display of a sub-frame of 50×50 pixels at 10Hz is desirable for acquisition/focusing.

4. 10 off slow auto-guiding detectors (to maintain alignment of optical train). 1Hz frame rate adequate. May use internal light sources rather than starlight, and may not be required at all if the path length compensation trolley tilt correction uses lookup tables instead of real time feedback (Section 12.2).

5. Fringe tracking detectors for 20 outputs of the pairwise beam combiner, operating at JHK with optimal sensitivity in H for faint sources. Each output has 5 spectral channels and is sampled twice per coherent integration time. For phase tracking, integration time is as short as 1ms, so a minimum of 10kHz pixel rate is required. For group delay tracking on the faintest sources read noise of $< 1.5e^-$ (possibly at a slower read rate) is required. $1e^-$ read noise would allow spatial filtering to be used to further enhance SNR.

6. IR science detectors: Need to detect $J/H/K$-band light coming from 8-12 outputs of the science beam combiners. Each output has up to 100 spectral channels and is sampled at up to 5kHz. Read noise $< 1e^-$ desirable for high-resolution modes. High quantum efficiency (typically $> 50\%$ in the relevant wavelength bands), good linearity, dark counts < 10/pixel/second, and dynamic range of $\sim 100 : 1$ are also required ($\sim 1000 : 1$ is preferred).

7. Detector readout must be synchronised with path modulation either actively or passively by time-tagging of samples. Active synchronisation is the preferred option.

8. Data from fringe detectors must be available for real-time analysis (e.g. for servo correction of paths). When the servo is running at the highest sampling rate the latency should not exceed $100\mu s$.

14.2 Proposed solution

14.2.1 Visible Wavelength Detectors

The L3 ("Low Light Level") technology now available from Texas Instruments and E2V Technologies (formerly Marconi/EEV) appears to be the ideal technology for the high-performance visible-wavelength detectors. It offers photon-counting performance, 15MHz pixel rates and dark noise below

the specified $10e^-$/pixel/second provided that the detectors are cooled below $-10°$C. Front illuminated detectors are already commercially available from both companies and E2V is now distributing samples of back-illuminated devices that offer bare silicon quantum efficiency.

The visible-light sensor needs can then be addressed as follows:

Tip tilt sensors: Avalanche photodiodes could in principle be used but have high failure rates. A more cost-effective solution in the long run is to use the E2V Technologies back-illuminated L3 detector, which has high quantum efficiency and blue sensitivity. Thermoelectric cooling is required to minimise noise. Eleven detectors, one per telescope and a spare, are required.

There are two additional advantages with this approach. Firstly, it allows access to a high magnification image at the telescope focus for alignment purposes. Secondly, if larger format devices become available in the near future the tip-tilt sensor can also be used as a finder camera.

Optical science combiners: While the quantum efficiency and fast readout requirements are similar to those of the tip-tilt, deeper cooling is recommended to reduce noise to an absolute minimum. One solution is to use liquid nitrogen cooling, in which case it may be possible to economise by placing several detectors in each dewar (use of mechanical refrigerators is *not* recommended due to vibration issues). Another is to use multi-stage thermoelectric cooling such as is already commercially available with some L3 cameras. However, in the latter instance care must be taken to minimise the effects of the dumped heat on internal seeing.

Finder cameras: A solution is available which is in the process of being installed into the COAST interferometer. It consists of a Starlight Xpress HX516 CCD camera and a PC-style single board computer at each telescope with custom software to allow flexibility of integration, binning, subframing and tracking signal output. Camera output can be viewed and controlled anywhere on the local network.

Technology in this field is moving very quickly, however, and the development of both L3 devices and network cameras should be monitored very closely over the next twelve months in the event that either use of tip-tilt detectors for acquisition becomes feasible or superior acquisition camera technology (that maintains the flexibility we require) becomes available.

Eleven cameras are required, one per telescope and a spare.

Slow autoguiding cameras: The Starlight Xpress is an available option here also. Whatever camera is chosen, one per telescope beam and a spare are required, so eleven off.

14.2.2 Infrared Detectors

No detector that meets our requirements is yet available. However, Rockwell Scientific are currently developing a range of HgCdTe arrays (called AOMUX) that are expected to have $1e^-$ read noise at high frame rates and with quantum efficiency in excess of 50% in J, H and K bands. Rockwell claims to have already demonstrated $< 5e^-$ readout noise reading out a 128×128 array at 1.5kHz (25MHz pixel rate) and expect to have $2e^-$ readout noise with a 6MHz pixel rate by December 2002. The operating temperature is specified as 80K so liquid nitrogen cooling will be necessary.

If we have one spectrum per chip our pixel rate requirement will only be ~ 500kHz for the science detectors. So for each required spectrum we could instead in principle read out fifty spectra at the full 25MHz rate and average them to get the noise down below $1e^-$ even with the chip in its current state of development. If there are two spectra per chip we could average 25 samples and still be below the $1e^-$ specified. However, either option would add significantly to the controller complexity and hence to development costs. It would be preferable to read out at the rate we require if that is feasible.

Expecting (but not assuming, see subsection 14.4) that these devices will be available in time to be incorporated into the MROI design, then, the following solutions are proposed:

Fringe tracker: Ten Rockwell detectors are required for the twenty spectra to be collected, as some economy can be achieved by placing two spectra on each detector. A spare is also required.

Science combiner: Although multiple spectra per detector are possible the necessary additional optics would add complexity and reduce photonic throughput. Hence we anticipate requiring up to one Rockwell detector per science beam, so 8 to 12 detectors depending on the design of the science beam combiner, and a spare.

14.3 Budget

It is difficult to price the infrared detectors at their current stage of development. This is also true of the cost of developing suitable controllers for them, as we have no information on the precise design of the electronics required to read the detectors out. However, based on previous experience with Rockwell's HAWAII chips we estimate that each detector will cost of the order of $50k, or $100k including controller electronics and cooling. Hence infrared detection is likely to be the most expensive aspect of detector development for the MROI. It may indeed be more economical to licence the AOMUX technology from Rockwell and do a fabrication run of these devices. One could then envisage the possibility of recouping some of the costs by manufacturing more devices than necessary and making the remainder available to the astronomical community.

The estimates below include our estimate of the cost of manufacture and assembly. The effort required for development is discussed in 14.3.2, below, and remains to be priced.

14.3.1 Equipment

Estimates of the costs associated with the detector subsystems are given below. The actual price of the IR detectors will depend on the level of volume discount available, but is likely to be much less than the $140k estimated price for a single one-off system. The variation in number of science detectors will depend on the precise details of the beam-combining optics. The cost of one additional spare detector has been included under each heading.

Item	Number required	Unit cost/k$	Total/k$
Tip tilt sensors	11	10–15	110 − 165
Optical science combiners	9 − 13	15	135 − 195
Finder cameras	11	2	22
Slow autoguiding cameras	11	2	22
IR Fringe tracker combiners	11	100	1100
IR science combiners	9 − 13	100	900 − 1300
Overall total			$2.3-2.4M

Table 10: Approximate costings for detectors for the MROI. A 10 telescope array has been assumed.

14.3.2 Staff costs

We estimate that it will require up to five man-years of effort to develop hardware and software for these devices. This excludes the costs of manufacture and assembly, which can be contracted out and are included in the above estimates. The development effort will need to be conducted by a specialist with experience in reading out infrared detectors.

14.4   Risks

Finder cameras and slow autoguiders make use of proven technology and have minimal associated risk. Risk associated with L3 detectors is also small, as they have been demonstrated to achieve the sensitivity and readout rates required. The infrared detectors pose the most risk due to their relatively early stage of development and their expense, but we are becoming increasingly optimistic that they will fulfill the requirements within the necessary timeframe. Furthermore, even this risk can be hedged: in the event that the AOMUX detectors will not become available, a commercially available Rockwell product (the PICNIC array) can be used, for which readout at the rates we require with $3e^-$ noise has been demonstrated. This would still allow the MROI to do excellent science in the infrared.

14.5   Questions for further study

1. Will the Rockwell AOMUX detector meet the needs of the MROI?

2. What other relevant array detector developments (such as large format L3 CCDs) might occur over the next year?

15   System Alignment

15.1   Requirements/issues

- Much of the optical path consists of relays of flat mirrors. These need to be aligned so that the shear of the centre of the stellar beam with respect to the centre of each mirror is no greater than a few mm otherwise light will be lost. This corresponds to arcsecond accuracy in some of the mirrors.

- Starlight which is centred on the fast tip-tilt trackers at the telescope must reach the beam combiners with less than 0.1 arcsecond tilt error with respect to a common fiducial.

- There must be a way of checking that the level of higher-order aberrations introduced by the optical system is less than $\lambda/20$.

- It should be possible to realign the system on a nightly basis or after a power failure without excessive requirements being placed on the operators.

- Initial alignment during commissioning should be as easy as possible.

- There should be a way of monitoring the throughput of the optical system on a nightly basis (or more frequently if possible).

15.2   Proposed solution

No real solution is presented here. Design for alignment should be an integral part of each subsystem and also a global concern. Routine alignment should be fully computerised and allow for alignment of all 10 optical trains in parallel, otherwise it will take too long and be too error-prone. This means that almost all optical mounts in the system should have motorised adjustments under computer control. Substantial cost savings could perhaps be made if there are no absolute position accuracy requirements on the motorised adjustments.

One suggestion is to follow the NPOI solution, which is to have a series of LEDs on mechanical mounts that pop into the beam train as an aid to automated mirror alignment at the start of the evening and are then removed for observing. There should also be internal light sources such as artificial stars and lasers as an aid to manual and automated alignment and testing when necessary.

It should be possible to mount a wavefront sensor, for example a 10×10 Shack-Hartmann system with $\lambda/100$ wavefront precision, at several points in the optical train to allow measurement of high-order wavefront errors.

15.3   Questions for further study

1. Suitable schemes for all the subsystems need to be designed.

2. Automation of these, and remote diagnosis of alignment errors needs to be designed in.

16 Control System

We need to develop an appropriate philosophy for designing and building the control system. A number of decisions need to be made with respect to the size of and division between subsystems, and the level of responsibility for integration that should be left to the controls team. With these questions in mind, here are three different approaches to building a control system for the MRO interferometer.

In general, the control system for the MRO Interferometer will consist of a central controlling unit, the Observatory Control System (OCS), and a number of subsystems which communicate with the OCS and possibly with each other.

1. **Small subsystems**. A subsystem could for example be (a) a delay line, (b) a fringe tracker, (c) a beam combiner, or (d) a telescope mount, and there will thus be much communication between the different subsystems that does not involve the OCS (e.g. to close servo loops). The controls group takes care of all the integration of subsystems. In this case much controls effort must be invested in order to interface all of the systems, both with each other and with the OCS. However the cost of producing each subsystem will be reduced because little controls work needs to be done by the subsystem contractor.

2. **Large subsystems without strict interfacing requirements**. Dividing the observatory into large subsystems means creating boundaries between subsystems such that the only communication that takes place outside a subsystem is with the OCS. This communication should be low-bandwidth (this to be defined), all high-bandwidth communication links being confined within individual subsystems.

   In this scenario the controls group is responsible for interfacing with each subsystem, but the subsystem contractor is responsible for interfacing the different components of the subsystem. There will be little requirement on how the subsystem communicates with the outside world, except perhaps that it should be through TTL-compatible digital signals. In Figure 15 the dotted line delineates a subsystem, and the boxes inside it are the components of the subsystem, which would be "small subsystems" in the philosophy outlined in (1). The controls group is only responsible for interfacing with the signals crossing the dotted box.

3. **Large subsystems with strict interfacing requirements**. In this case each subsystem (defined as in (2)) must conform to a particular protocol. How this is achieved internal to the subsystem is up to the subsystem contractor.

16.1 Requirements/issues

- The observatory should be able to operate all night without human intervention, except for fault conditions, and possibly adverse weather conditions.

- It should be possible to control the entire observatory from a single terminal, probably running a graphical operator interface. When this should be achieved remains open (i.e. at turn-on, or several years later?).

- It should be simple to install the operator interface on a new computer. The interface should be a client of the control system, and should communicate with it via a standard network protocol (probably TCP/IP), and at low bandwidth (56K baud or whatever will be standard low bandwidth at turn-on). Control of the array should not be limited to a particular terminal in the control room. It should be possible to perform routine operation via a low-bandwidth link.

- Hierarchical alarms should be implemented. A few top-level alarms alert the operator to errors without providing overwhelming amounts of information. Alarms may be opened in a tree-like structure to reveal more details in order to quickly and accurately pinpoint problems.
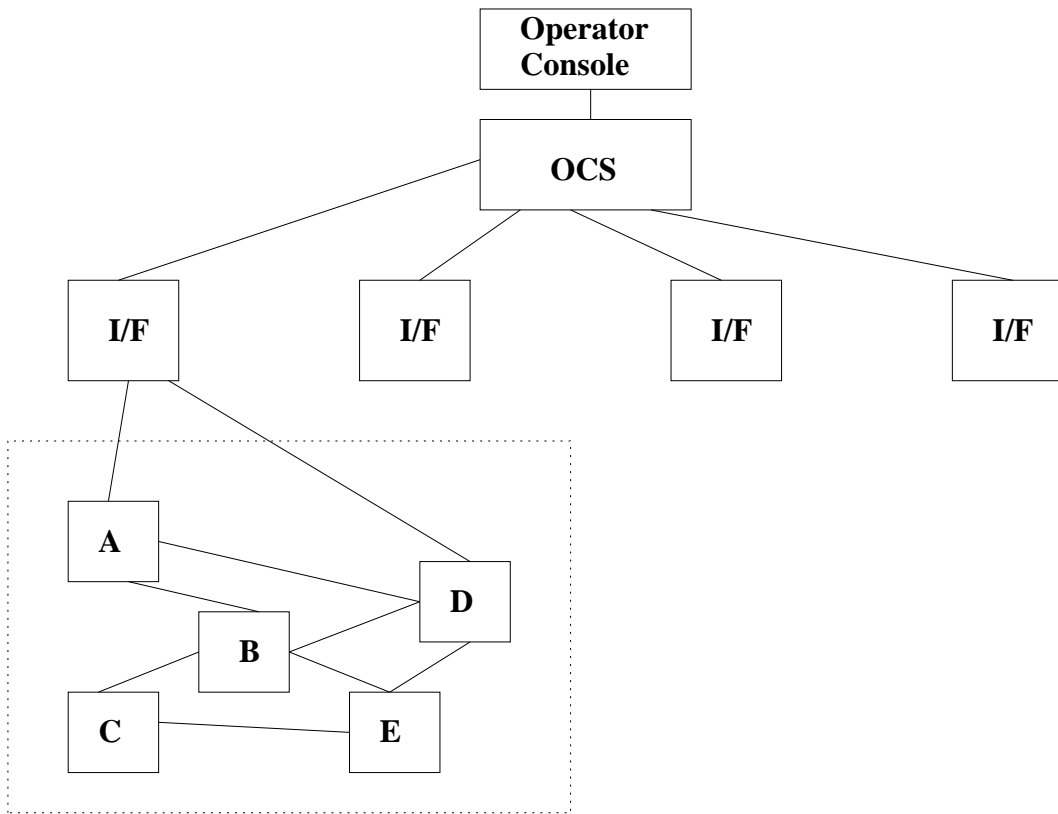
Figure 15: Illustration of large subsystems with loosely-defined interfaces. The boxes labelled "I/F" are computers whose function is to interface the OCS with a particular subsystem.

- It should be possible to follow observing in read-only mode at a remote location. The client program should be available for installation at a remote site in read-only mode.

- A limited amount of near real-time data analysis should be provided. This should be sufficient to judge how well the system is performing scientifically.

- OCS testing should be built in. Simulators should be available for all major or critical subsystems. This will allow testing of the OCS by simulating fault conditions in some subsystems. Initial simulators may be quite rudimentary.

- Subsystems should work autonomously where this makes sense. It should be possible to operate a subsystem in a useful manner even if no other subsystems are functioning.

- Computers should be located in one room whenever possible. This allows for easy operator access during the night for diagnostics and repair. This computer room should be located in the same building as the control room.

16.1.1 Control system lifetime

Regardless of what system we choose for building the control system, we should expect that it will need to be rewritten completely on a timescale of 5 years. Recent history tells us that few computer packages have a lifetime longer than 5 years. New versions of the software will require newer hardware, and updating older versions of the hardware will require modern software. With an anticipated lifetime of the observatory of 20 years, the control system should undergo 4 life cycles. The design should anticipate this.

16.2 Meeting the Requirements

16.2.1 Organization of the controls group

The controls group should be staffed with controls engineers. MRO scientists should generally not write the control system, except for defining top-level science requirements, or when there is a scientific rationale for working on specific aspects of the control system. One organization that has been suggested is that of a scientist overseeing a group of skilled controls engineers.

16.2.2 Personnel resources

The personnel resources required to build the control system depends heavily on which philosophy is chosen. To a large extent, the philosophy chosen impacts how risk and responsibility are distributed, and whether personnel resources are budgeted with the individual subsystems or with the control system.

Scenario 1: The entire controls and subsystem integration effort is budgeted under the controls group. In this case the estimated effort is 12 people for 4 years.

Scenario 2: Integration of subsystem components is budgeted in each subsystem, and the controls group is only responsible for communication between the OCS and each subsystem, as well as for the interfacing of each subsystem with the OCS. In this case the estimated effort is 8 people for 4 years.

Scenario 3: Integration of subsystem components as well as interfacing of subsystems with the OCS is budgeted under each subsystem. The controls group is only responsible for writing the OCS itself. In this case the estimated effort is 2 people for 4 years.

With the educational component of MRO, it may be appropriate to exchange some of the controls engineers with engineering students. This increases the personnel pool, but decreases the per person skill level.

16.3 Example MROI control system

This section outlines an example control architecture for the MROI. We have assumed the small subsystems model in order to illustrate the level of complexity required in an interferometer array of this nature. This complexity does not go away in the other scenarios, it is just "hidden" in boxes that are not the direct responsibility of the controls team.

We have also assumed:

- An EPICS-based control system

- A particular design for the array, which is broadly that described in this document. Where details are unspecified in the current system design we have made fairly arbitrary decisions in order to present a concrete example

In EPICS-speak, hardware is interfaced to Input-Output Controllers (IOCs), which use the Channel Access protocol to communicate with each other and with other CPUs (Channel Access clients, or CA clients for short) on the EPICS network.

16.4 Control architecture

Figure 16 illustrates an EPICS-based control architecture for the MROI. As EPICS cannot handle real-time communication or high data rates, the control architecture includes CPUs that communicate using other protocols (not defined here). These CPUs also run EPICS for the purpose of non-real-time communication, where this would be useful.

For many of the boxes identified as Input Output Controllers (IOCs) in Figure 16, it will be impossible to interface a single CPU to all of the intended hardware. In these cases several physical IOCs will be used. However, the logical structure of the control system can remain as outlined here. One such sharing of hardware control among several CPUs *is* drawn on the diagram: the trolley control IOC sending real-time path corrections to a CPU that controls a piezo actuator.

The components in the diagram are described in the sub-sections below. The diagram does not show every communication link between IOCs/CA clients. The action sequences in Section 16.5 hopefully illustrate that drawing all of the links would render the diagram unreadable! Non-EPICS data links are shown, as are EPICS links that operate at $\geq$1Hz (it turns out these are all involved in servo systems).

16.4.1 Observatory Control System (OCS)

This is a Channel Access (CA) client, responsible for coordinating the operation of the entire interferometer array.

16.4.2 Telescope Control System (TCS)

We envisage a separate control system for each telescope in the array. Each telescope has its own CA client (labelled TCS in Figure 16) that communicates with the IOC CPUs for that telescope:

- **Motor Control System (MCS)**: interfaces to the telescope drives and encoders (for both the primary/secondary assembly and for the tertiary mirror) and the secondary mirror actuators; responsible for tracking and slewing the telescope

- **Finder**: interfaces to the finder CCD camera and corresponding display hardware. Sends correction signals to the MCS at ∼1Hz during acquisition

- **Tip-tilt**: interfaces to the tip-tilt detector and the actuators for tip-tilt correction (assumed to be on the tertiary)
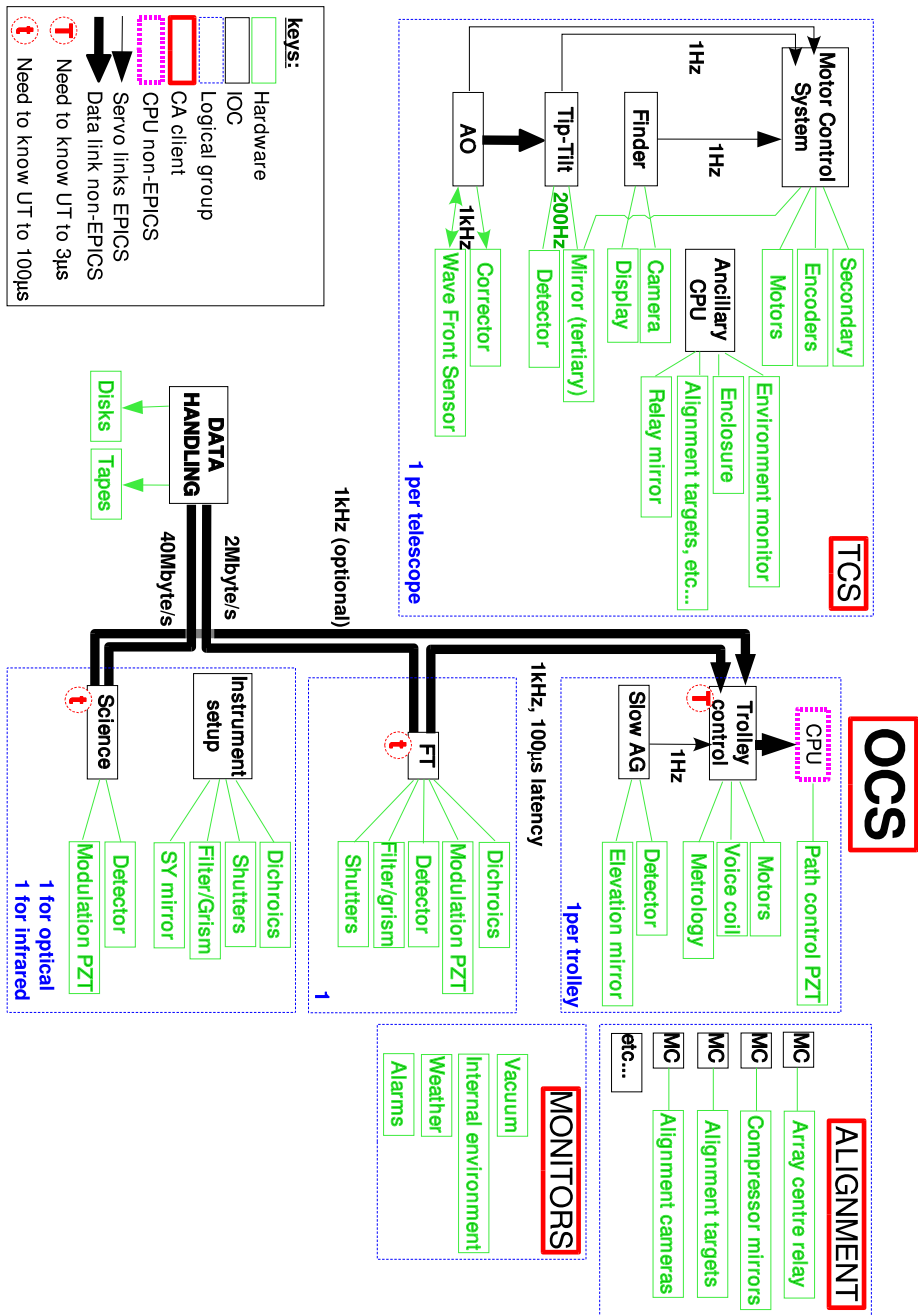
Figure 16: Proposed control architecture. See text for further explanation.

- **Adaptive Optics (AO)**: interfaces to the wavefront sensor and corrector. The data link between the AO and tip-tilt IOCs is for the transmission of tip-tilt corrections obtained from the AO wavefront sensor, which will be corrected by the active mirror in the tip-tilt system

- **Ancillary CPU**: interfaces to the hardware for environmental monitoring at the telescope, operating the telescope enclosure, inserting/removing alignment targets, and adjusting/inserting/removing the relay mirror (in the vacuum pipe near the telescope)

16.4.3   Trolley control

We have assumed that the servo system for correction of geometric and atmospheric path delays is a three stage system, with the actuators for each trolley (in order of decreasing throw) being:

1. Trolley drive motor

2. Voice coil

3. Piezo stack (may be necessary for phase tracking)

Each trolley has its own "trolley control" IOC. The OCS is responsible for setting the absolute positions of the trolleys within the pipe (only the relative positions are constrained by the need to obtain fringes on all baselines).

The slow autoguider is responsible for maintaining the alignment of the beam trains in the presence of thermal drifts and azimuth errors associated with the trolley rails (assuming a roof mirror retro-reflector). Azimuth error signals are sent at 1Hz to the trolley control system, and elevation corrections are made using an separate mirror.

16.4.4   Fringe Tracker (FT)

A single IOC is responsible for operating the entire fringe-tracking system, which must work co-operatively to estimate $N - 1$ (where N is the number of telescopes) atmospheric path delays from a possibly different number of fringe patterns.

The estimated delays are communicated to the trolley control IOC at $\sim$1kHz (via a dedicated link), as part of the delay correction servo.

16.4.5   Science beam combiner

There are two pairs of "instrument setup" and "science" IOCs — one pair for the optical beam combiner, and another for the infrared combiner.

Instrument setup   This IOC interfaces to the hardware for configuring the beam switch-yard, controlling the beam shutters, and inserting/removing filters, grisms, pinholes etc. into/out of the light paths within the science beam combiner.

Science (fringe sensor)   This IOC operates the science array detector and the corresponding path modulators (the operation of these components must be synchronised).

16.4.6   Data handling

This IOC is responsible for archiving the raw data from the fringe tracking and science combiners, as well as for automated (but non-real-time) reduction of the data. The primary data links (thick black lines in Figure 16) are non-EPICS, but averaged (i.e. low bandwidth) versions of the data will be available via EPICS, e.g. for the automated alignment.

16.4.7 Alignment

The alignment CA client coordinates the actions of a (currently undefined) number of IOCs. These interface to the hardware required for automatic alignment (actuators, pop-up targets, detectors,...) that is not connected to one of the IOCs mentioned previously.

16.4.8 Monitors

This CA client communicates with the IOCs for monitoring of the pressure in the vacuum system, the internal environment (temperature, humidity,...), weather. There is also an IOC that can sound sirens when human action is urgently required!

The vacuum pumps and valves are not under computer control for safety reasons.

16.5 Action sequences

The most important sequences of actions to be performed by the MROI are illustrated in Figures 17 and 18. These sequences should be the only ones needed for automatic service observing (with telescope operators on site).

Some explanatory notes are given below. Otherwise, it should be possible to identify the hardware and IOCs associated with a particular action by reference to Section 16.4 above.

Only paths taken if actions succeed are shown. Some "decision" points are marked in Figure 17, but further discussion of error handling procedures is beyond the scope of this document.

16.5.1 Observing queue

We have assumed that an observing queue is set up before the start of each night, specifying all required parameters. These include target object, (constraints on?) time of observation, calibrator stars, science and fringe-tracking wavebands, spectral dispersion, fringe-tracking mode, observing mode (i.e. how much data, which baselines/triangles). This would require input from both the proposal authors and the telescope operators.

This type of queue does not require intelligent processing i.e. decisions to be made automatically during the night about what to observe, based on the seeing, preliminary measurements etc. Such a facility could be added later, but would no doubt require many extra man-years of effort.

16.5.2 Startup

The diagram (Figure 18) outlines the actions that are carried out automatically at the start of the night. This excludes daytime maintenance tasks such as pumping down the vacuum system and filling dewars with liquid nitrogen ("liquid nitrogen check" means check that there is sufficient LN2 to last the night).

We envisage two alignment procedures: a pre-sunset alignment of everything inside the building (we assume thermal effects will not normally necessitate re-alignment of these components after sunset — there must be a "quick check" routine to determine whether this is the case on a given night), and a post-sunset alignment of the "outdoor" components. The details of the alignment schemes have not been designed yet.

Performing a pointing model or baseline solution requires observing about six stars well-distributed over the sky. The pointing model only needs the stars to be acquired; the baseline solution requires fringes to be found on each. The same stars can be used for both procedures, to increase efficiency.
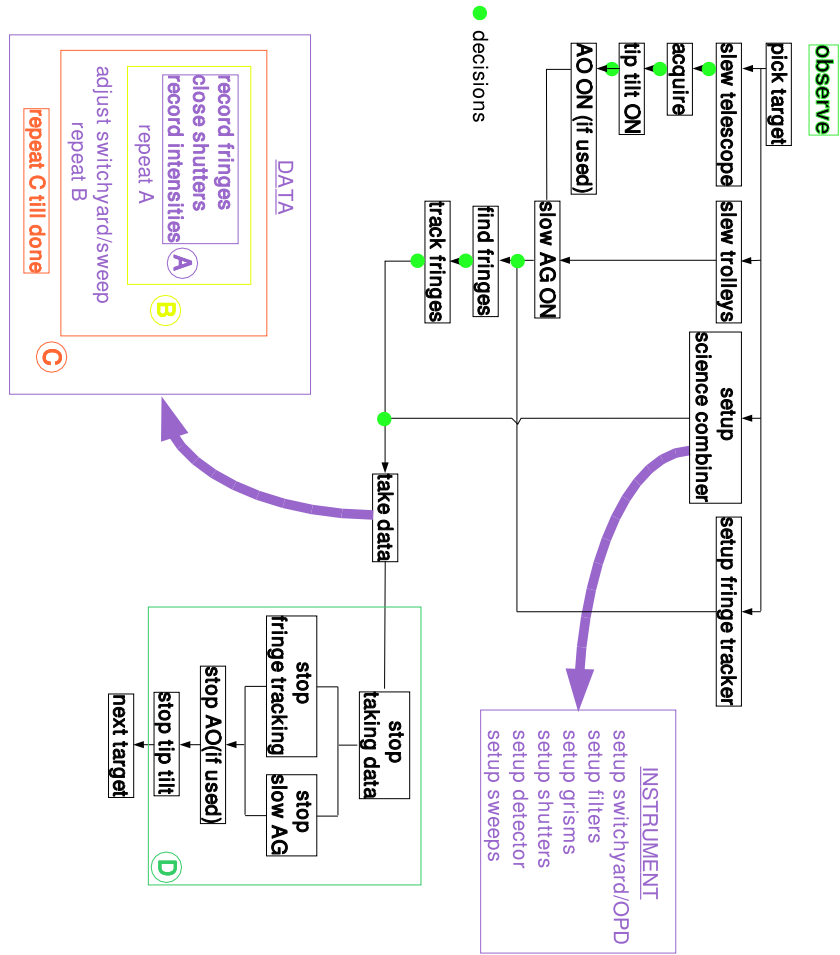
Figure 17: Action sequences for observing. See text for explanatory notes.

startup

environment control off
self test OCS/IOCs
liquid nitrogen check
check observation list
pre sunset alignment

sunset

check weather
open domes
post sunset alignment
start observing

shutdown

stop observing (see (D) in observe list)
park telescopes
close domes
"stow" all systems

"off" system
environmental control on

telescopes
delay lines
AO
tip tilt
detector shutters

alignment reference setup

science beam → angles
combiner   shears   mirrors   grisms/feeds
+switchyard   paths   spatial filters

fringe tracking → angles
beam combiner   shears
                 paths
                 differential path

beam compressors
slow AG
delay lines

quick check of (A)
relay mirrors (vacuum)
tip-tilt system
finder
AO system (if used)
telescope optics inc secondary/tertiary
fringes off flats
pointing model/baseline solution ●
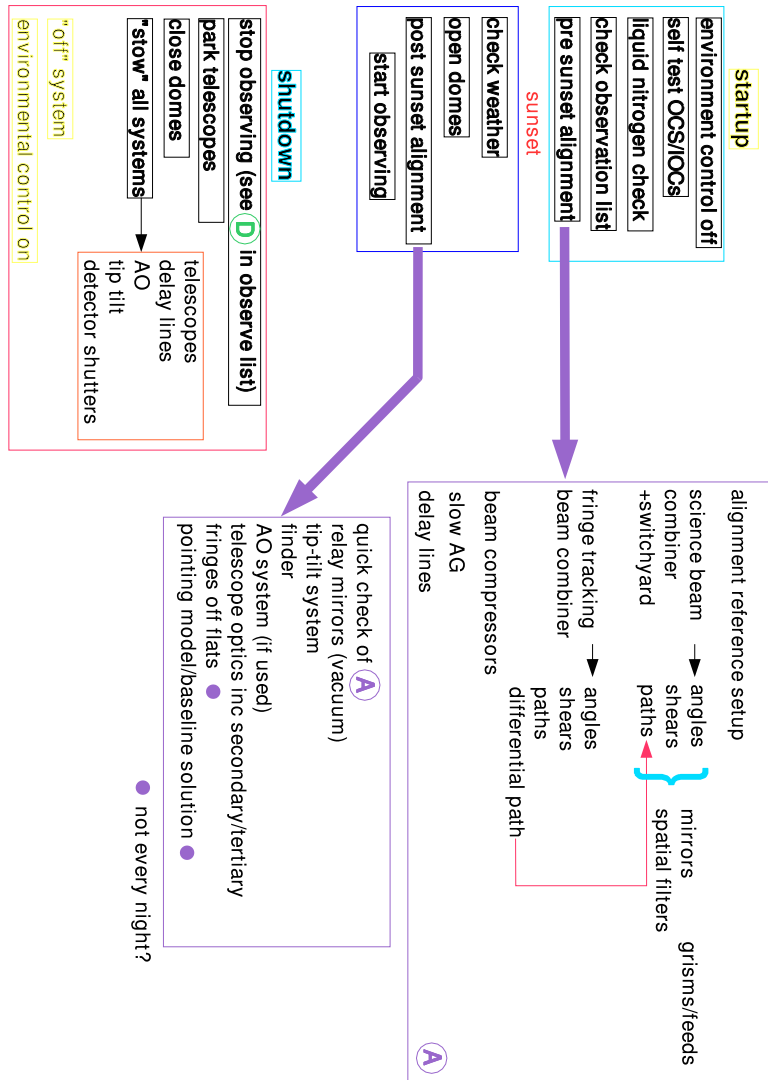
● not every night?

(A)

Figure 18: Action sequences for array startup and shutdown. See text for explanatory notes.

60

16.5.3 Shutdown

Two tasks need clarification here. To "stow" a subsystem is to put it into a state where it can safely be left for up to a few hours. For example, this may involve moving components into a position where they are protected from dust, or where a subsequent power failure would not damage them. It should not take more than a few minutes to bring a system to readiness from the "stowed" state.

To switch "off" a subsystem is to put it into its daytime state (which may or may not involve switching off the power).

We propose three variations on the shutdown procedure:

- Normal shutdown, as illustrated in Figure 18

- Emergency shutdown, which does not wait for observing tasks to finish cleanly

- Sleep mode, used e.g. while waiting for clouds to pass. Here the subsystems are "stowed" but not switched "off".

16.5.4 Observing

The actions in Figure 17 are hopefully transparent. The "decision" points marked are where the control system decides whether to proceed based on the success or failure of previous actions. Apart from this element, the scheduler illustrated is completely dumb — it just works its way though a sequence of observing targets, performing a fixed set of actions (defined in the observing queue) for each.

16.6 Budget

A typical controls engineer costs roughly \$125K/year at NMT.

Scenario 1: Small subsystems. Effort 12 people for 4 years, or 48 man years. \$2M in hardware for interfacing. Total cost \$8M.

Scenario 2: Loose large subsystems. Effort 8 people for 4 years, or 32 man years. \$1M in hardware for interfacing. Total cost \$5M.

Scenario 3: Tight large subsystems. Effort 2 people for 4 years, or 8 man years. \$250K in hardware for interfacing. Total cost \$1.25M.

16.7 Potential Compromises

Choosing large subsystems over small subsystems involves a tradeoff. Large subsystems involve less effort by the controls group. On the other hand, they are more complex, and are more at risk of being delayed, which could make commissioning of the array difficult. Also, because much of the controls burden is placed on the subsystem builder, the cost of the subsystem is greater.

Smaller subsystems involve a greater and more complex effort by the controls group, with an associated risk of increased cost and delays. On the other hand the subsystems are simpler, making prompt delivery easier, and reducing cost since the controls burden is placed on the controls group.

We currently favor scenario (2), large subsystems without strict interfacing. Large subsystems are preferred to minimise in-house staffing needs. The loose-interfacing model has the advantage over scenario (3) that the MRO controls group has an interface computer for each subsystem within its remit. If a subsystem is modified, this can in many cases be compensated for by re-programming the interface computer, leaving the control system unchanged. Secondly, the interface computer can be used to simulate the subsystem for testing purposes, even before the subsystem is delivered.

16.8   Questions for further study

It is well recognized that there may be cost/vendor issues with the favored "large subsystems" model for the control system, but it provides a "straw-man" to compare and contrast against. The main advantage of this approach is that it reduces the need for in-house staffing, the potential drawback is higher direct subsystem cost.

A decision will need to be made on what system we will eventually use to build the control system. Will it be coded from the ground up? Will we use EPICS? Will we use VxWorks? RTLinux? QNX? These decisions should be left to the engineers who will design the final control system. However, in the meantime there are several directions that we can research.

We should visit other interferometers and draw on the experience of COAST. What we want to know is what they would do today if they were building their control system with the knowledge that they now have. We should also attempt to understand the negative experience that some parts of the VLTI community apparently have had with EPICS.

17 Observation preparation and data reduction

17.1 Requirements/issues

The following sections review a number of the key issues associated with the preparation of observations at the MROI and requirements for data reduction software.

Observation preparation

- An important aspect of the MROI observing model is that we envisage service observing, i.e. it is not expected that astronomers will visit the site for observing.

- In this case, astronomers will need to specify the appropriate array configuration, observing wavebands, spectral dispersion, observing mode (one of diameter measurement, snapshot image, high-fidelity image etc.), and seeing requirements, before the observation is queued.

- Appropriate calibrator stars must also be selected — there are potentially a number of persons who might be responsible for this.

- Finally, we will need to consider the question of training. Who will provide support and training for astronomers using the facility?

Data reduction

- As well as observation preparation tools, there must be a standardized pipeline to deliver calibrated visibility amplitudes and closure phases.

- Thereafter, astronomers will be expected to be responsible for producing their own images from these data, as, for example, at the VLA.

- Nevertheless, tools to produce images from the calibrated data, and to fit models in the uv plane, must be made available.

17.2 Proposed solution

We are proposing to use resources supplied by others wherever possible. In particular, existing software to prepare observations (e.g. getCal from the JPL/NASA Interferometry Science Center and ASPRO from the ESO community) could be utilised with little effort. We need not provide a complete electronic proposal-submission system initially.

ESO has an extensive programme to measure diameters of calibrator stars and to develop catalogues and expert systems to facilitate the selection of calibrators for a particular observation. The US Interferometry Science Center is also deploying considerable effort in this area. We expect that several publicly-available calibrator catalogues and calibrator selection tools will be available on the timescale needed for MROI.

The data reduction pipeline will be fairly instrument-specific, and so must be custom-written. However, this work will draw on the Cambridge experience of writing equivalent software for COAST. We will be able to minimise coding effort by making extensive use of high-level scripting languages for which we have many years of experience.

The calibrated visibility amplitudes and closure phases will be supplied to the astronomer in the OI Exchange format (http://www.mrao.cam.ac.uk/~jsy1001/exchange/) currently being developed under the auspices of the IAU.

Collaborative efforts to develop mapping and model-fitting software have already begun in the optical interferometry community. Eric Thiébaut (JMMC & AIRI/CRAL, France) has developed an

image reconstruction package, aimed at the VLTI, that would be suitable for MROI and is already producing good results. Similar software (BSMEM) is being worked on in Cambridge, as is a Bayesian model-fitting program. We anticipate that by the time MROI becomes operational, software that can be straightforwardly adapted to our requirements will have been written and debugged.

17.3   Questions for further study

Continued effort is needed to ensure that the IAU-coordinated software effort works for us. However, this should be straightforward as a number of the COAST team (JSY/DFB) are heavily involved in this initiative.

18 Information management

Information management is not data management (data management is discussed elsewhere). The information referred to in this section includes project communications (e-mail, problem reports, working group communications, meeting minutes), light schedule information (events and meetings calendar), documents (publications, image archive, procedures, requirements and specifications), as well as public information.

18.1 Requirements/issues

We require a system in which information (as defined above) is readily available for viewing and for modification by anyone who has a need to do so. At the same time we require a modest level of security to prevent casual access to those who should not be accessing certain information in certain ways.

18.2 Meeting the requirements

This set of requirements is very similar to the requirements that the Sloan Digital Sky Survey (SDSS) had when they started operating. The solution adopted by the SDSS was to organize a few web servers where the information is maintained. The SDSS requirements are somewhat more strict and formalized than those of the MRO. The SDSS facility is an operational facility with fixed procedures, and large amounts of daily formal communications. However, initially organizing ourselves in a similar fashion, and then relaxing the procedures where appropriate may be a good way of proceeding.

The proposal is for an inexpensive ($2K) web server. The server is in fact currently operational, and can be found at http://mro.nmt.edu. It is owned by LANL but hosted at NMT. To ensure maximum availability, a second server (which is currently at LANL) will be installed and the system will be mirrored to it so that a switch can be performed quickly in case of a system failure.

The server will include a public web site, which will be the official web site for MRO, and a password-protected internal web site. The public site should be maintained primarily by a Public Relations professional. It will contain news releases, archived and real-time images from the ridge, and background information on the science.

The internal web site will contain the following items:

- Calendars. This calendar system will contain schedules of events and meetings. It is not meant as a formal scheduling calendar for the construction activities, but rather an informal calendar system for the consortium members. Editing the calendars takes place through a web-based interface.

- Meeting minutes. This will be a place to post minutes of all MRO meetings.

- Mailing list server. This will serve as an archive for e-mailed information within the MRO. There will be general mailing lists, and lists for specific activities and sub-groups.

- Problem reports server. We will need a way of tracking problem reports and other action items within the MRO project. The server should be able to receive new problem reports (PRs), allow for assigning them to appropriate personnel, handle approvals when needed, and track progress on a PR to solution.

- Reference information. This includes contact information for MRO members and contractors, How-To documents, and requirements and specifications for the observatory systems.

- Document archive. This includes refereed and non-refereed publications, a photo archive, web pages and documents related to various working groups.

The initial setup of this server is currently underway. Anders Jorgensen's time paid by LANL is spent on this task. Once completed, the server should be handed over to a systems administrator for day-to-day maintenance. We expect these maintenance duties to require approximately 30% time of a systems administrator.

18.3   Questions for further study

Proper information management should facilitate the work in the project. It should not become a burden to perform for project members. We need to continuously monitor usage of our system and make it as user-friendly as possible.

19 Interferometer infrastructure

The interferometer will need the following buildings:

1. A beam combining lab which includes the $\sim 200\,\mathrm{m}$ delay line tunnel. This should be grass covered if possible & as close to the centre of the array as practicable. A smoothly curved roof is desirable.

2. A nearby control room from which the array will be operated.

3. A shed for a telescope and its transporter.
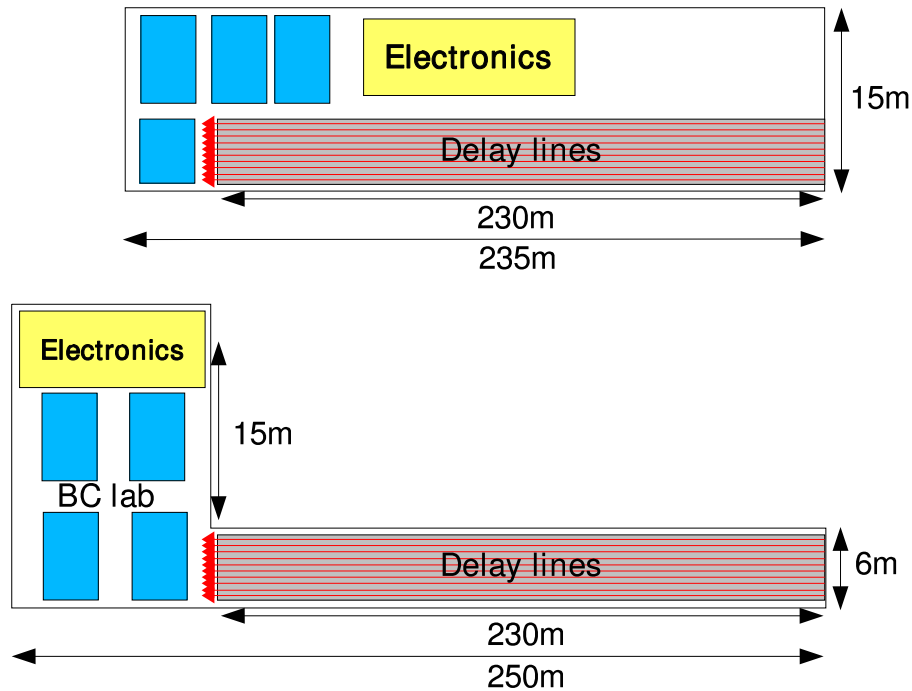
Figure 19: Two alternative layouts for the beam-combining lab. In both cases the long axis of the building is parallel to one arm of the interferometer and the beams enter from the left hand side. The dimensions assume a $400\,\mathrm{m}$ maximum baseline and $75\,\mathrm{mm}$ diameter beams.

A vehicle capable of safely picking-up and moving a telescope and cover is required, together with the appropriate roads or tracks needed to move a telescope to new foundations. A coating facility for mirrors up to 1.4m is needed either on-site or close enough by to make regular re-coating possible. This could be at the NM Tech campus.

Services required include:

1. Electrical power: Estimate a few kw per telescope plus 20kW for the main optics lab. Total 30–50kW.

2. Generators or some way of making the array safe without mains power. (May be sufficient to close each telescope cover.)

3. Water - modest amounts for coolers etc, but these are all recirculating.

4. Liquid nitrogen. Estimate 10 litres per detector dewar per day, so perhaps 100 litres of liquid nitrogen total per day.

5. A network link at 10MB/s.

6. Air conditioning. The use of this should be minimized - passive thermal management is preferred wherever possible.

At each foundation we need: a kinematic base, the beam transport vacuum pipe end, 2 phase mains and Ethernet (fiber optic for lightning protection). There needs to be room to move and install the telescope and its cover.

20   General infrastructure

Even though the Magdalena Ridge site has been used for decades by the Langmuir Research Center, their utility support is marginal at best, and new utility support must be supplied for MRO. This will entail new electric power transmission, new propane storage, a new water supply, new sewage and waste disposal, new communication links, and new fire control and emergency facilities.

A major new control center/administration building is required, complete with offices, meeting rooms, labs, control rooms, kitchen facilities, rest areas, a physical plant, equipment and vehicle storage, and parking. Separate buildings will be needed for an electrical sub-station, general storage, and a southern site rest and support facility for the interferometer staff. Water storage, for both potable and fire water, is needed, as well as propane storage for building heating. A potable water treatment system will likely also be required.

All on-site utilities will be distributed underground to preserve the site air flow/seeing, and to reduce the visual impact of the site. Road access to the Langmuir Center and the west knoll towers must be preserved though re-routing of the roads should be acceptable.

Fire protection for our structures must be provided with cognizance of ignition sources both from our local operations and from the surrounding forest. Provision must be included to protect the National Forest from fires generated by MRO. In this regard, the USFS has requested the MRO provide at least 120,000 gallons of on-site stored water for fire control.

Hanta virus is present in the site rodent population and appropriate steps must be taken to minimize exposure to such risks.

All of these above facilities must be generated with minimal disturbance to the existing drainage patterns and conscience control of possible erosion. Environmental considerations will dictate design and construction that minimalizes the visual impact of structures and avoids disturbance of the Mexican Spotted Owl.

20.1   Requirements

The general basis for infrastructure requirements is to provide electrical and water needs for the estimated maximum and continuous populations resulting from Langmuir, MRO itself, NMT usages, and USFS visitors. Langmuir will continue to rely on its own backup power and waste facilities. Previous discussions have set the maximum site population at 70 with a long term continuous load from 10 people.

This project is to provide infrastructure for all planned aspects of the project and reasonably foreseeable expansions. The buildings are to be expandable should major new developments dictate.

There is no appropriate water supply near the ridge top, so a water well will be developed in the valley west of the mountain and water will be pumped to the site. Pressure considerations will require multiple lift stations (3) along the utility route. It is planned to bury the water line and include new electrical lines and copper and fiber communication lines in the same excavated trench. There are currently two alternative utility routes for this trench and final route selection awaits soil and ground stability data as well as cost estimates.

A summary of infrastructure needs follows:

Electrical Usage (440 volt max local, much higher voltage in transmission lines up mountain.)

- Building lighting and local usage
- HVAC
- Water supply and treatment
- Fire pumps (also with standby power source)
- Science needs

- Observatories
- Telescopes
- Science bldg. loads

Propane storage

- 120 days for heating, distributed in multiple tanks near buildings.

Potable Water

- Average usage
- Peak usage
- Storage

Fire Water

- Storage
- Distribution rate

Sanitary Sewage

- By local septic systems to handle occupancy. (rejected an option to pipe sewage down mountain for off site treatment)

Solid waste

- Removal by truck from local storage (Dumpsters)

Communication Links

- Copper and fiber in utility trench
- Other comm. as dictated by science needs TBD

Snow removal

- Large snowplow to be stored at/near physical plant area
  Expect regular plowing during winter months
- Snow mobiles for local emergency transportation

Hazardous Material Handling

- Schedule Haz. Mat. Operations off site.
- Local loads to be handled by septic systems and less than janitorial loads.

Emergency Handling

- First aid center in Control Center building
- Fast access for ambulance
- Helicopter Landing area for emergency transport

Backup Power Supply

- By propane or diesel powered generator to provide orderly shutdown, emergency occupation, and fire pump loads.

General Storage

- Admin. Bldg. labs and P plant:

  5000 sq. ft. separate storage building including room for telescope mover storage and an extra telescope foundation

20.2 Budget

A summary of the estimated budget and its breakdown is given below:

Control Center/Admin. Bldg. 18,600 sq. ft. @ $150/sq.ft.	$2,800,000
Util. Corr. + pumps/well	$3,000,000
Storage bldg.	$100,000
Elect. Drop Bldg.	$150,000
South site hut	$100,000
Util. local distribution	$500,000
Water Tanks	$200,000
Backup generators	$100,000
Water Treatment	$100,000
Roads/Walks	$200,000
Septics	$30,000
Propane Storage	$20,000
TOTAL GENERAL INFRASTRUCTURE	$7.3M

20.3 Unresolved problems

1. Choice of utility corridor

2. Location of South Hut

3. Location of storage bldg./is size adequate?

4. Water Tank burial $\sim$ 200 meters from balloon hanger?

5. Haul water instead of pumping?

6. Location of water treatment facility

7. Hanta Virus needs

8. Rest area sound control

9. Main bldg. traffic flow vis-a-vis room locations

10. Optimum location of electric sub-station

11. Main Bldg. roof access

12. Gate rebuild?

13. Radio noise reduction, both for Langmuir and for CCD cameras: HVAC, Motors, computers, control boards

14. Road grader/bulldozer/snowplow

15. Telephone/communications

16. Bury Electrical drop bldg?

17. Safety: Construction, operational

18. On-site utility trenches

19. On-site roads and walkways

21 Technical risks assessment

In order to limit the technical risk associated with the project as a whole, the design we are proposing capitalizes on many of the innovations that have been developed at other interferometers worldwide. Some of these are summarised below.

Subsystem	Task	Arrays with closest experience applicable to the MROI
Array configuration	Layout	NPOI, CHARA, VLTI
Unit telescopes	Design	CHARA, COAST
Adaptive optics	Design	COAST
Beam transport	Vacuum	NPOI, SUSI
	Dispersion	GI2T, NPOI, SUSI
Delay lines	Trolleys & rails	CHARA, COAST, NPOI, SUSI
Beam combination	Combiners	CHARA, COAST, NPOI
Detectors	Array detectors	COAST, IOTA, PTI
	Spectrometers	COAST, PTI, NPOI, SUSI
System alignment	Long baselines	CHARA, NPOI, SUSI
Array control	All aspects	CHARA, NPOI, PTI
Observing preparation	All aspects	KECK, PTI, VLTI
Infrastructure	All aspects	CHARA, NPOI

It is clear from the above that MROI can draw upon existing experience to a great extent. The principal challenge for the project will be integrating together this experience into a coherent whole, and optimizing each system so that the overall package delivers the top-level science goals. We have excellent relations with the teams working on the arrays mentioned above and so we can realistically expect to benefit greatly from their accumulated knowledge.

A   A Science Case for the MRO Interferometer

The following is a provisional science case for the proposed interferometer to be built at the Magdalena Ridge Observatory (MRO) in New Mexico. It is broadly based on the science case for the Large Optical Array, a facility array that was proposed for development by the UK between 1998 and 2000, but has been augmented to cater for some additional science interests of the MROC members. The LOA project did not receive funding due to the UK's decision to join the European Southern Observatory. However, it was highly ranked scientifically, just beneath requests to fund access to ESO, ALMA and NGST.

A.1   The need for an imaging array

Interferometry offers the only route to reach the angular resolutions required to provide direct and detailed observational constraints of many fundamental astrophysical phenomena. In simple cases, where the physics is thought to be well understood, a single measurement may suffice, e.g. measuring the angular diameter of a hot star. However, for most problems, our picture is at best rudimentary, and in many instances even the basic geometry is in doubt. The only way forward will be to image the object reliably and in detail with the appropriate angular and spectral resolution. The unique science of the MROI will come from its capability to do *model-independent* imaging of a wide range of astrophysical phenomena. An important result of this emphasis on imaging is that the results from the MROI will be accessible to a broad audience, which is in keeping with the educational goals of the array.

A very wide range of possible scientific projects is possible with an imaging interferometer with angular resolutions on the order of a milliarcsecond and operating at visible and near-IR wavelengths. Within that broad capability three major themes in contemporary astrophysics have been identified as core programmes. All of these exploit the unique imaging capability of the MROI. We summarize these areas below:

1. **Star and planet formation:** the detection and characterization of protostellar disks. Accretion, disk-clearing, fragmentation and stellar duplicity over all mass ranges. The role of angular momentum in star formation.

2. **Stellar evolution:** mass loss and accretion via winds, jets, outflows, and Roche-lobe overflow. Studies of examples in single and binary systems in themselves and as analogs for AGN jets and beams.

3. **Active galactic nuclei:** resolved imaging of the nuclear dust component of AGN, the broad-line-region (BLR), synchrotron jets and nuclear and extra-nuclear starbursts.

The following sections describe these fields in some more detail.

A.2   Imaging the birth of stars and planets

The birth of stars is of central importance to astrophysics whilst the formation of planets is of fundamental interest to mankind at large. These phenomena are inextricably linked since planets form out of the material left over from the star formation process. New stars form when clouds of interstellar gas and dust (sub-micron sized particulates) collapse due to their own gravity. The initial angular momentum of the clouds inevitably leads to the infalling material taking up a flattened, rotating configuration. The physical mechanisms controlling the accretion onto the new star via this disk lie at the heart of star formation. Once most of the material has accreted onto the star, gravity takes over in the remnant disk itself and it is here where planets condense out to form new solar systems.

The HST has been able to reveal the outer regions (>10 AU, i.e. ten times the Earth-Sun distance) of accretion discs around new stars, and future arrays of millimetre-wave telescopes will analyse the physical conditions there. The MROI on the other hand will be able to probe within 1 AU, where Earth-like planets are found in our own Solar System. Images from the MROI will provide our first direct views of the processes feeding planet formation around other stars. The census of extra-solar planets grows year by year, but there is no substitute for an understanding of their formation process. Only then will we be able to extrapolate across the Galaxy to predict how many planetary systems must be present.

A.2.1 Discs, gaps, and accretion flows

Young stars still settling down to hydrogen nuclear burning, and with masses similar to the Sun, are known as T Tauri stars. The many hundreds identified are almost all brighter than 14th magnitude and located at quite modest distances, e.g. in the Taurus cloud at a distance of ∼140 parsec. Even before the HST had resolved their outer regions, the presence of circumstellar accretion discs had been inferred from excess emission at infrared wavelengths. These discs' luminosity is made up of two components, the greater typically being a passive component due to the absorption/reemission or scattering of stellar radiation, and the lesser, an intrinsic component radiated as infalling material gives up gravitational energy. The MROI will have the sensitivity to image the thermal dust emission from such discs out to a diameter of around 0.2 AU at $2\,\mu$m, where the apparent diameter of the discs will be 2 milliarcseconds for sources 100 pc away. At shorter wavelengths, scattered starlight from the disc will predominate and is expected to be detectable out to significantly larger diameters.

Theories of star formation predict that strong magnetic fields in young solar-type stars disrupt the inner accretion disc at around $5 - 10$ stellar radii and that the material completes its journey to the star via magnetically-channeled arcs (e.g. Hartmann et al. 1994). This has been proposed to explain a lack of near-infrared emission from the hot inner disc in some objects, and the presence of red-shifted absorption lines, indicative of infalling material, in others. These structures are predicted to be visible on milliarcsecond scales and so will only be directly observable using the long baseline configuration planned for the MROI. Indeed this is a major science driver for the MROI and it has been designed to look directly for holes in the continuum emission. In addition, its spectral capability will allow imaging in emission lines that may very well reveal accretion arcs looping out of the disc plane. A time series of Hα images will reveal the rotation rates of these accretion arcs and provide a direct measure of the shear forces involved. The unique snapshot imaging capability of the MROI will be crucial for this type of study. The existence of such magnetospherically-controlled structures has important consequences for the subsequent rotation rates of stars, which in turn drive their stellar dynamos, for disc clearing, and thus for the formation of the inner planets. Their confirmation, or otherwise, would represent a fundamental advance in our understanding of star and planet formation.

Gaps and holes in circumstellar discs are also predicted to be formed by companion objects, whether in the form of stars or planets. A large body of theoretical work links the resulting disc structures, e.g. annular gaps, spiral waves, and accretion streams, to the properties of the satellite object and those of the disc. To date, however, only a limited number of wide multiple systems have been imaged (e.g. Monin & Bouvier 2000; McCabe et al. 2002). This leaves the small milliarcsecond scales, on which we can study the effects of new planetary companions on the disc structure, entirely unexplored. Although few extra-solar planets are likely to be luminous enough to be directly visible with the MROI, they will be revealed by the readily detectable ∼0.1 AU wide 'grooves' in the disc that they create during their formation. As before, the indirect evidence for gaps inferred from the spectral energy distributions of young stars is subject to many model uncertainties (Jensen & Mathieu 1997). By imaging possible accretion streams linking the planet to the disc, the MROI will be able to determine whether planets and stellar companions can continue to grow in mass once they have carved a gap in the surrounding disc.

The formation of solar-type stars and other 'solar systems' is of obvious importance. However, there is also great astrophysical interest in the formation of stars much more massive than the Sun.
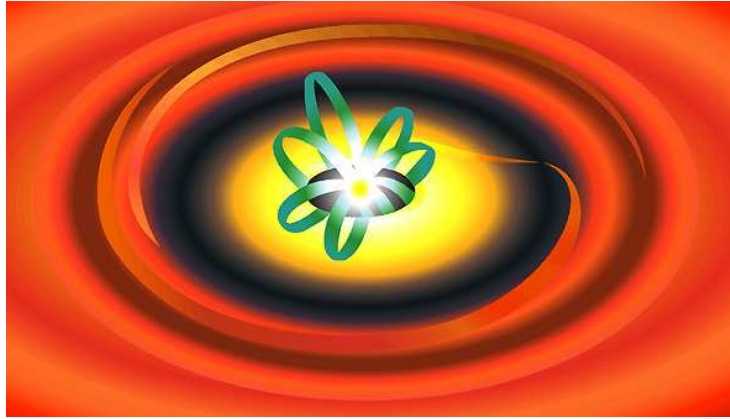
Figure 20: Artist's impression of a young star with a circumstellar disc and protoplanet, based on current ideas derived from unresolved observations. The dark annular gap has been swept out by the protoplanet, located at a radius similar to that of Venus, whilst the inner edge of the disc is truncated by the star's magnetic field at a distance somewhat smaller than Mercury's orbit. Within this region material falls onto the star via magnetized streamers. The MROI will be the first instrument able to resolve the central hole and the accretion arcs, and detect planets via the gaps and spiral streams generated in the disc.

Importantly, these hot luminous stars are responsible for a wide range of energetic phenomena that in turn regulate ongoing star formation in our own and other galaxies. The circumstellar environments of the known higher mass young stars (Herbig Ae/Be stars and less heavily obscured BN-type objects) remain the subject of controversy, not least because of the surprising outcome of the limited interferometry carried out with IOTA (Millan-Gabet et al 2001) that suggests disks around Herbig stars may be rare – other results such as derived from spectropolarimetric data (Vink et al 2002) suggest otherwise. This comes at a time when views on how higher mass stars form remain divergent (cf Bonnell et al 1998 and Behrend & Maeder 2001). Along with these more luminous young stars, T Tauri stars undergoing bursts of enhanced accretion (FU Orionis systems) will be important targets for and resolvable by MROI on the ≤ 1 AU scale. We anticipate several dozen such targets. Astronomers will be able to map out the emissivities of discs or other structures in both emission lines and continuum on sub-milliarcsecond scales. Velocity-resolved spectral line images will remove the need for simplifying assumptions, e.g. Keplerian motion, and allow direct physical interpretation of their measurements.

A.2.2 Jets and outflows

It is clear that the MROI will provide a massive step forward in our understanding of the physical processes governing infall onto new stars. However, a significant component of current star formation research is concerned with comprehending the numerous observations of outflow phenomena from young stars, such as jets, winds and bipolar flows. These flows are an integral part of the star formation process and may be important for carrying away the huge excess of angular momentum that has to be removed before stars can form at all. Several theories have been proposed to explain the driving and collimation of these flows, mostly involving a magnetohydrodynamic mechanism, but a consensus is still some way off. The MROI will be able to image the very origin of the highly-collimated ionized jets from low mass young stars, in prime diagnostic emission lines such as Hα, the HeI 1.083 μm and 2.058 μm lines and the CO first-overtone bands at 2.3 μm. This will provide a critical test of models such as the 'X-wind' and related pictures (Shu et al. 1994, Uzdensky et al 2002) which seat the origin of the wind at the well-defined corotation radius between disc and star (i.e. the inner edge of the disc in these models, resolvable by the MROI). The observed morphology of the base of the jet will determine exactly where the collimation takes place and provide vital clues to the mechanism responsible.

Different mechanisms are suspected to be responsible for the outflows from more massive young stars, where radiation pressure may dominate over the effects of magnetic fields (e.g. Hollenbach et al. 1994; Drew et al. 1998). Little evidence for stellar jets is seen, with high resolution radio observations suggesting a predominantly equatorial morphology for the ionized flow on 100 milliarcsecond scales (Hoare et al. 1996). It should be possible to use high angular resolution studies in strong HI emission lines to discriminate between disc photoevaporation models (which posit line emission on a scale of several AU, ~ 10 milliarcseconds in Orion) and direct disc mass loss scenarios, where radiation pressure drives material directly off the disc surface close to the star (~ 0.1 AU), i.e. at the resolution limit of the MROI.

A.2.3 Residual dust discs

The MROI is expected to play a ground-breaking role in studies of residual dusty debris discs around young main-sequence stars, of the sort epitomised by Vega and β Pic. Relatively few of these systems have imaged to date (e.g. Marsh et al. 2002; Weinberger et al. 1999), often using coronagraphic methods, so that no information on the innermost disk regions is available. Most inferences about the properties of these regions are therefore based on radiative transfer fits to the disk infrared energy distributions, which suggest that the warmest particles are located a few AU or less from the stars, corresponding to angular separations that range from 1-15 milliarcseconds for many systems. The MROI has the potential to directly image the discs on these scales. As in the case of T Tauri stars, an obvious role will be to search for annular gaps, as evidence for particle shepherding by planets in Earth-type orbits.

A.2.4 Uncovering low-mass companions to cool stars

Measurements obtained using a variety of techniques have shown that at least 50% of stars form in multiple systems. However the methods employed to date have not yet been able to explore the full range of possible brightesses and separations. An important role for the MROI will be to explore multiplicity in a much wider range of environments than has been possible to date.

As well as detecting companions with *much* smaller angular separations (e.g. <10 AU in Taurus), The MROI will also allow the characterisation of those systems already discovered by spectroscopic or lunar occultation techniques (Mathieu 1994; Simon et al. 1995). The MROI will also be able to follow the orbital motion of these objects thereby allowing dynamical mass determinations. This would be a crucial step in calibrating evolutionary tracks, which are extremely uncertain for pre-main sequence objects, brown dwarfs and planets. With spectral resolutions of approximately 200 in the IJHK bandpasses it will also be possible to perform compositional analyses as a function of mass, allowing a direct comparison with atmospheric models.

The MROI offers the prospect of directly detecting substellar companions. Spectroscopic surveys of nearby solar-type stars have revealed the presence of a number of close companions that may be giant planets or brown dwarfs (Delfosse et al. 1998) . During the pre-main sequence phase, even planets are relatively hot and luminous and would be within the MROI's capability to detect (Burrows et al. 1997). Spectroscopic follow-up observations of these companions will be able to confirm their substellar/planetary status. The MROI will also be a powerful tool for studying older substellar objects. For example it will just be sensitive enough to search for *companions* to the brown dwarf GJ 229B ($\sim$1000 K, $\sim$0.04 M$\odot$) which lies at a distance of 5.7pc and has an age of 1-5 Gyr (Nakajima et al. 1995; Allard et al. 1996). Precision radial velocity measurements and the all-sky infrared surveys (DENIS & 2MASS, e.g. Reid et al. 1998) mean that there are a rapidly growing number of low-mass stellar and sub-stellar objects to add to the many existing binaries whose study is beyond current technology.

The information that the MROI will provide on the multiplicity of low-mass objects will be essential for determining the low-mass end of the stellar mass function. Since the majority of objects are in

multiple systems, companion-star luminosity and mass ratios are crucial for the reliable determination of the overall mass function. Present measurements of M dwarf and brown dwarf masses have only been feasible for a small number of systems in a limited region of parameter space (systems with angular separations >0.1 arcsecond and orbital periods <20 yrs can be studied) yet the uncertainties in the correction for unresolved binarity can lead to orders of magnitude differences in deduced space densities (Reid & Gizis 1997, Kroupa 1998). Once again, observations with the MROI have the potential to revolutionize this field.

A.2.5   The role of angular momentum

There has been limited progress in solving the angular momentum problem identified by Spitzer (1968). Basically, the angular momentum of a protostellar cloud due to galactic rotation and equipartition is 10^4 to 10^6 times greater than the angular momentum of a typical star of the same mass. There must be a torque that slows the rotation of the cloud. The exact nature of this torque remains elusive. In an associated problem, we have limited knowledge of the relative importance of global angular momentum and turbulence in the formation of star clusters.

The missing ingredient required to make significant headway in these problems is the ability to measure the angular momenta of significant samples of stars in clusters. With conventional techniques the only observable quantity is $v \sin i$, where v is the rotational velocity and i is the inclination to the line of sight. It is very difficult to separate v from $\sin i$, and the orientation of the angular momentum vector is completely undetermined. An imaging interferometer with a spectral resolution of order 30,000 to 50,000 would allow determination of all these quantities in stars of F type and earlier. It would also determine when there is significant differential surface rotation: the velocity field obtained when a stellar disk is resolved can be analyzed for shear with well known techniques from 21-cm radio astronomy, e.g. van der Kruit & Allen (1978).

Observations of nearby clusters such as the Ursa Major Moving Cluster should allow determination of the correlation of the directions of the rotation axes of stars in the cluster. A large correlation would imply that angular momentum is dominant over turbulence in the formation of these clusters and *vice versa*; this would be first step in applying such analyses to a range of cluster types including star-forming regions in Taurus.

A.3   The life-cycle of stars

For the majority of their lives ($\sim 10^{10}$ years for a star like the Sun) stars burn hydrogen in a quiescent core. After this fuel is exhausted, core nuclear burning progresses on to helium-burning and a carbon-oxygen core develops. A phase of catastrophic mass loss then ensues, during which as much as 80% of the total mass of the star can be ejected into space. One of the major aims of the MROI will be to uncover the physical processes underlying this catastrophic mass loss, which remains the least understood phase of stellar evolution.

This mass-loss phase, when the star is observable as an extreme red giant, is of crucial importance to the formation of further generations of stars. The ejected material is enriched by the products of nuclear burning, especially nitrogen and carbon (oxygen and heavier elements mainly come from supernovae) and in addition, dust and organic molecules form in the ejecta. Furthermore, there is now growing evidence that planets can form in the ejecta around the dying star, a previously unsuspected phase of planet formation. Interestingly, enrichment is also of major importance in the early evolution of the Universe, since the presence of dust causes increasing obscuration in quasars and young galaxies.

A.3.1   The physics of mass loss

Mass loss in extreme red giants is believed to be driven by a multi-stage process. Initially, pulsations and convection extend the stellar atmosphere by very large factors > 100%. At the cooler outer edges

of the atmosphere, silicate or carbon dust can then begin to form. Finally, radiation pressure on the newly formed dust causes it to flow out, dragging the gas with it.

Our main uncertainties lie with the first step: neither the structure of the extended atmosphere nor that of the star are understood. Stars at this late stage of their evolution are largely convective (and possibly chaotic) and their surfaces are believed to be dominated by a relatively small number (≤ 50) of giant convective cells. In addition, they can also pulsate strongly, but neither the cause of the pulsations nor their effects on the atmosphere, through for example, shock waves, are well understood. Even for the nearest such stars, the stellar surface and dust-formation radius extend to only 10-100 milliarcseconds, so that detailed studies require the angular resolution that only the MROI will provide.

Optical interferometric studies (Tuthill et al. 1997) have already shown that the nearest evolved stars have asymmetric surface structures (hot-spots) containing up to 10% of the total flux from the stars. The MROI will allow astronomers to make detailed surface maps of these stars for the first time, revealing the structures and temperatures of the hot-spots as well as their possible identification with convective cells. Establishing the topology of the cells, i.e. whether they form latitudinal rotational bands or banana-shaped segments along lines of equal longitude, as well as defining their timescales, will represent major leaps in our understanding of convection, a notoriously difficult problem.

A.3.2 Dynamical studies

In cool evolved stars, the spectrum of the stellar atmosphere is dominated by deep opaque molecular absorption bands, especially those of TiO. The photospheric layers at the wavelengths of these bands, i.e. the depths to which we can look, are therefore high up in the extended atmosphere in these cases. By mapping in bands of various optical depth, as well as in the infrared continuum, depth-mapping of the stellar atmosphere becomes possible. This will allow convective cells traveling upwards through the atmosphere to be tracked. Evidence from observations of molecular masers suggests that the region of dust formation shows clumps of higher density. These may be related to the convective structures below, or they may trace dynamical instabilities in the circumstellar environment. Since the dust is assumed to form at temperatures close to 1000K it will be possible to image it in the near-infrared K-band. Images from the MROI will thus enable astronomers to create 3-d maps of the atmosphere and to relate the structures seen to the hot spots on the stellar surface.

One crucial dynamical experiment will be to image the pulsational motion of the outer layers of these evolved systems directly. For Mira variables this will lead to crucial tests of non-linear models for stellar pulsation, which otherwise cannot be tested straightforwardly. For Cepheids (more luminous systems) this will provide a unique method for establishing their distances by combining radial velocity measurements with the angular diameter variations. This will only be possible using the long baseline capability of the MROI and promises a new independent calibration of the Cosmic distance scale.

Another key experiment will be to image shock structures in the pulsation zone using different wavelengths. Ionized regions will be delineated by Hα emission, whereas H$_2$ and CO emission should trace the post-shock zones. Astronomers using the MROI will thus be able to determine whether dust forms in the post-shock regions as postulated by the Vienna and Berlin groups (e.g. Hron et al. 1998; Fleischer et al. 1995). Neither of these models include the effects of upwardly mobile convective cells, and so monitoring observations with the MROI are likely to test them severely.

On larger angular scales there is evidence for strong anisotropy in the mass motion, i.e. the spectacular bipolar outflows observed at the end of mass loss. These structures are amplified by interacting winds of different velocities, but their actual cause is unknown. The MROI will be the only instrument capable of imaging at sufficient resolution to study the effects of companions on mass loss processes.

A.3.3 Mass-loss in binary systems

The study of interacting binaries forms a second major topic following this evolutionary theme where the MROI is likely to have a major impact. Systems such as classical novae, recurrent novae and

symbiotic stars, and atmospheric eclipsing binaries will be imaged by the MROI for the first time.

Classical novae are very close binary systems in which a red dwarf is paired with an accreting degenerate companion. Occasional explosions, thought to be due to thermonuclear runaways on the white dwarf, characterise the nova activity. These are ideal laboratories for studying mass accretion onto compact objects as well as the physics of thermonuclear runaways. The ejections are so energetic that spectroscopic measurements indicate that velocities as high as 1000 km/s can be attained. At best, radio observations can image the ejecta 80 days after the outburst. Observations with the MROI, on the other hand, will be able to spatially resolve the optical and NIR emission from the ejecta only a few hours after an outburst. Around three nova outbursts are expected to be observable each year, offering many opportunities for detailed study. At later phases multi-wavelength imaging by the MROI will detail the shock structure in the ejecta and for the first time show if dust formation is associated with them.

Recurrent Novae and Symbiotic Stars are much wider systems where the mass-donating star is a red giant/Mira variable. There are 12 recurrent novae and 200 symbiotic systems known which the MROI will be able to detect and resolve. Their orbital periods range from 200-1000 days, and so at 1000 pc typical binary separations will be 10 milliarcseconds. The binary separation and orbital parameters, the nature of the companion, the wind ionization geometry and the accretion disk geometry will all be observable with the MROI through imaging of the continuum and line emission. Radio data indicate that UV radiation from the white dwarf/sub-dwarf ionizes the molecular wind from the red giant. The MROI will be able to relate the radio emission directly to the location of the binary components for the first time. For some recurrent novae an accretion disk may also be present around the companion. Measurements with the MROI would then track the evolution of the shock structures caused by the passage of the companion, thus testing and enhancing our current models of astrophysical shocks.

One final class of system observable with the MROI will be the atmospheric eclipsing binaries. These consist of an evolved M giant star and a much hotter B-type main sequence companion with a typical period of 8 to 20 years. The stars may share a tenuous circumbinary envelope and there is some evidence that an accretion disk may also surround the B-star. Mass transfer from the M-star to the B-star is non-uniform: spectral line studies suggest that inhomogeneous structures (convective cells/thermal instabilities) in the M-star photosphere are the starting point for dense molecular clumps which then flow from the M-type star and accrete onto its partner. These molecular clumps will be detected and imaged by the MROI in many such systems. The MROI will thus be able to confirm this model of accretion by directly tracking the clumps from the M-star surface to the B-star, and furthermore will show how the pulsation modes of the evolved M-stars are affected by its hotter companion.

A.4   Imaging the hearts of active galaxies and quasars

The cores of active galaxies (AGN) and quasars, where gas and dust are believed to be spiralling in towards a massive black-hole, are some of the most energetic and enigmatic objects in the Universe. However, despite their importance, our knowledge of them has had to come indirectly, through e.g. spatially unresolved spectroscopy and variability studies of their broad emission lines and their optical/ultraviolet and X-ray continuum. Their large distances have meant that, apart from radio bright objects that can be probed using radio interferometry, few have had their cores imaged with any spatial resolution. Our detailed knowledge of these fundamental components of the Universe remains very sketchy. The MROI will be unique in allowing astronomers to image the very central regions of AGN in great detail without relying on the presence of a bright radio core. The MROI will exploit the very compact continuum source (and the broad-line region in more distant objects) to provide a reference instead, thereby opening a new window into those regions where the most energetic phenomena are taking place.
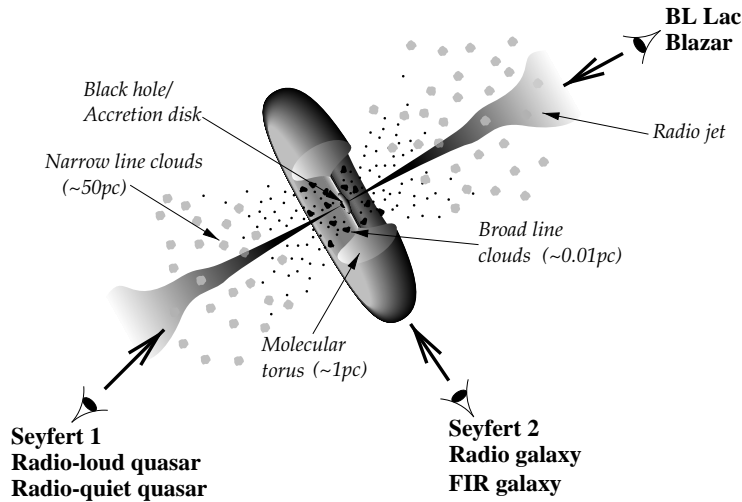
Figure 21: Schematic cartoon of the central regions of an active galaxy inferred from indirect measurements. The numbers in parentheses refer to distances from the central black-hole (at $z = 0.01$, $1\,\mathrm{pc} \simeq 20$ milliarcseconds). Depending on viewing angle the system shows significantly different observational characteristics. Many of the components listed have never been imaged directly.

A.4.1 The broad-line region - BLR

This zone, the origin of the broad emission lines seen in many AGN, is a fundamental component of active galaxy models. The techniques of reverberation mapping have shown that the BLR in Seyfert 1 galaxies has an extended structure whose luminosity-weighted radius is a few light-weeks for the Balmer lines (see, e.g. Peterson et al. 1991), but very little else is known about its geometry. For nearby AGN the scale of the BLR will be comparable to the proposed angular resolution of the MROI — at $z = 0.01$ a radius of 1 light-month corresponds to 0.2 milliarcsecond. Thus, for the lowest redshift, and hence brighter, objects, the MROI should be able to measure the size and shape of the BLR directly. It is unlikely that the BLR has a hard edge, and so fainter emission may be detected on larger scales than reverberation mapping methods can sample. One outstanding project will be to image the BLR in the Hα line with coarse velocity resolution. This will constrain the kinematics of the emitting plasma, and hence address the long standing question of the relative importance of turbulent bulk motions and rotation. Furthermore, long-term monitoring of the BLR may be able to associate flux variations in the BLR with changes in its detailed spatial distribution. This would be an outstanding breakthrough in understanding the dynamics of AGN cores.

A.4.2 The obscuring torus

The existence of giant dusty molecular tori surrounding the cores of active galaxies is indirectly supported by spectroscopy and spectropolarimetry, and is invoked to explain the division of AGN into two classes: Seyfert 1 galaxies and quasars (in which the nuclear continuum and BLR are visible directly) and Seyfert 2 and narrow-line radio galaxies (where these components can be seen only in scattered light). However, despite being central to the favoured AGN paradigm none of these tori has ever been imaged directly. Because they are dusty and heated by the central continuum source, they are ideally detected in the near infrared. Their inner edges are predicted to be roughly 1 pc from the nucleus (a limit set by the distance that dust grains can exist before they evaporate) which corresponds to 20 milliarcsec at $z = 0.01$, well within the MROI's resolution. A useful test-case is that of NGC 1068 which has a core K magnitude of 9.3, a factor of 80 brighter than the MROI's limiting sensitivity. Modelling

by Efstathiou et al. (1995) predicts an inner radius for the torus of 10 mas, with near-infrared thermal emission originating from a region at least a few times that size, depending on the details of the hot dust distribution. This will be easily resolvable with the MROI.

The key questions for astronomers to address with the MROI will be:

- Does the torus really exist? If we do not detect it with the MROI, then a fundamental revision of our current model of AGN will be needed.

- What is its geometry? Is it homogeneous or composed of many large discrete molecular clouds?

- How does the torus geometry depend on source luminosity? For example, hydromagnetic wind models predict that geometrically thick tori cannot form in high-luminosity objects. This is an important question since it could explain the absence of narrow line quasars.

- What is the temperature profile of the torus? This can be estimated from observations at several IR wavelengths, and, in principle, could be used to distinguish between the presence of a torus, or an inner warped disc.

A.4.3 The inner narrow-line region - NLR

Further out from the nuclear core, the MROI will be able to investigate the boundary region between the BLR and the more extended ionized plasma characterized by much narrower emission lines, the so-called narrow-line region. Although the NLR extends out to many arcseconds from the central engine, i.e. several 100's of parsecs, its innermost regions have never been resolved even with HST. In this intermediate zone, the roles for the MROI will be to establish both how the inner NLR connects to the obscuring torus, and to determine its structure and kinematics. For example, is it jet-like or disc-like on small scales? Imaging with the MROI's milliarcsecond resolution will be the ideal method to address these questions.

A.4.4 Jets and the radio-loud/radio-quiet dichotomy

Relativistic jets emitting radio synchrotron radiation are seen in all radio-loud active galaxies and (at a much lower level) in some radio-quiet systems. The brightest of these are also detectable at optical wavelengths. These extremely energetic jets, comprising beams of ultra-relativistic particles, exhibit a range of peculiar properties, for example apparent faster-than-light motion in blazars where the jets are pointed almost directly towards us. This type of phenomenon can only be seen on milliarcsecond scales and in the past has only been detectable at radio wavelengths using very long baseline interferometry (VLBI). With its comparable resolution in the near infrared and optical bands, the MROI thus has the potential to make significant and unique inroads here. Infrared and optical observations will provide important complementary information, since the radiating electrons have much higher energies than those emitting in the radio band and much smaller regions remain optically thin. For sources with bright compact cores, the MROI will be able to follow the evolution of components as they propagate along the jets. A comparison with simultaneous VLBI observations will then provide important new constraints on particle acceleration and energy-loss processes in the outflowing fluid.

In addition, the MROI may be able to elucidate the differences between radio-loud and radio-quiet objects. There is a clear association between galaxy type and radio loudness: radio-loud objects are found mostly in elliptical galaxies and radio-quiet objects in spirals. This difference must, however, be established on scales comparable with those of the parsec-scale jets. There is no consensus on the reason for this, but the MROI will be the only instrument capable of looking for differences in environment between radio-loud and quiet objects on these small angular scales.

A.4.5 AGN overview

Because of their large distances from us, observations of AGN will be among the most challenging for astronomers using the MROI. However, the extreme physics taking place in the cores of these sources means that the gains to be had will be spectacular. The most basic and important elements of our current AGN models, e.g. the molecular torus and the BLR, have never been imaged before, yet the MROI has the sensitivity and angular resolution to make that possible now. We know from radio VLBI that structures do exist on milliarcsecond scales in AGN cores: the MROI offers us the opportunity to study those in detail for the very first time at optical and near-infrared wavelengths.

One final point concerns sensitivity: recent observations with the NICMOS camera on HST have shown that a significant number of nearby AGN have nuclei which are bright enough to be observed with the MROI. For example, Kulkarni et al. (1998) show that there is an unresolved $K = 12.9$ source in the nearby Seyfert 2 galaxy IC5063 and Schreier et al. (1998) find $K = 10.5$ for the core of the radio galaxy Centaurus A. These new results suggest that there will be many tens of nearby AGN, together with a similar number of quasars and a few BL Lac objects in outburst detectable with the MROI. Resolved images of any one of these would represent a remarkable breakthrough.

A.5   Other programmes

The sections above give a flavour of the range of astrophysics that a carefully designed interferometric array could attack, and is certainly not exhaustive. Most have capitalized on the combination of sensitivity, resolution and imaging capability, that mark the MROI as a unique and innovative instrument, way ahead of competitor arrays.

However, as well as the core projects outlined here, the MROI will also be suited to the full range of programmes that other first-generation arrays have identified as scientifically important. These include, for example, the determination of fundamental stellar parameters (masses and radii), the investigation of limb-darkening on main sequence stars, and the study of motions in compact stellar clusters. In addition to these, important serendipitous targets, such as supernovae in nearby galaxies, which occur infrequently but which are of fundamental significance, will also be observed.

What is clear is that the scientific remit of a second-generation array such as the MROI will be very broad indeed, and will undoubtedly lead to fundamental advances in our understanding of numerous astrophysical phenomena. Observations with the MROI will encompass all the key areas of modern astrophysics including radiation processes, dynamical phenomena, accretion, star-formation, and jet-physics both within and beyond our Galaxy. Surveys, temporal monitoring and individual targeted observations will all be possible.

In the past improvements in sensitivity or resolution have led to major advances in astrophysics. By offering a factor of 100 improvement over the angular resolution of the HST, the MROI is certain to lead to ground-breaking new science.

References

[1] Allard, F., Hauschildt, P.H., Baraffe, I., Chabrier, G., "Synthetic Spectra and Mass Determination of the Brown Dwarf GL 229B", Astrophysical Journal, 465, L123 (1996).

[2] Behrend, R., Maeder, A., "Formation of massive stars by growing accretion rate", Astronomy and Astrophysics, 373, 190 (2001).

[3] Bonnell, I.A., Bate, M.R., Zinnecker, H., "On the formation of massive stars", Monthly Notices of the Royal Astronomical Society, 298, 93 (1998)

[4] Burrows, A., Marley, M., Hubbard, W.B., Lunine, J.I., Guillot, T., Saumon, D., Freedman, R., Sudarsky, D., Sharp, C., "A Non-gray Theory of Extrasolar Giant Planets and Brown Dwarfs", Astrophysical Journal, 491, 856 (1997).

[5] Delfosse X., Forveille T., Perrier C., Mayor M., "Rotation and chromospheric activity in field M dwarfs", Astronomy and Astrophysics, 331, 581 (1998).

[6] Drew, J.E., Proga, D., Stone, J.M., "A radiation-driven disk wind model for massive young stellar objects", Monthly Notices of the Royal Astronomical Society, 296, L6 (1998)

[7] Efstathiou, A., Hough, J.H., Young, S., "A model for the infrared continuum spectrum of NGC 1068", Monthly Notices of the Royal Astronomical Society, 277, 1134 (1995).

[8] Fleischer, A.J., Gauger, A., Sedlmayr, E., "Circumstellar dust shells around long-period variables", Astronomy and Astrophysics, 297, 543 (1995).

[9] Hartmann, L., Hewett, R., Calvet, N., "Magnetospheric accretion models for T Tauri stars. 1: Balmer line profiles without rotation", Astrophysical Journal, 426, 669 (1994).

[10] Henry T., Franz, O., Wasserman, L., Benedict, G.F., Shelus, P., Ianna, P., Kirkpatrick, J.D., Mccarthy, D., "The Mass-Luminosity Relation at the End of the Main Sequence", Astronomy and Astrophysics Supplement Series, 191, 4406 (1997).

[11] Hoare, M.G., Muxlow, T.B., "MERLIN observations of luminous young stellar objects", Astronomical Society of the Pacific Conference Series, 93, 47 (1996).

[12] Hollenbach, D., Johnstone, D., Lizano, S., Shu, F., "Photoevaporation of disks around massive stars and application to ultracompact H II regions", Astrophysical Journal, 428, 654 (1994).

[13] Hron, J., Loidl, R., Hoefner, S., Jorgensen, U.G., Aringer, B., Kerschbaum, F., "ISO-SWS spectra of the C-rich AGB star R Scl and dynamical model atmospheres", Astronomy and Astrophysics, 335, L69-L72 (1998).

[14] Jensen, E.L.N, Mathieu, R.D., "Evidence for cleared regions in the disks round pre-main-sequence spectroscopic binaries", Astronomical Journal, 114, 301 (1997).

[15] Kroupa, P., "On the binary properties and the spatial and kinematical distribution of young stars", Monthly Notices of the Royal Astronomical Society, 298, 231 (1998).

[16] Kroupa P., "The stellar mass function", Astronomical Society of the Pacific Conference Series, 134, 483, eds Rebolo, R., Marin, E.L, Zapatero Osorio, M.R. (1998).

[17] Kulkarni, V., et al., "Unveiling the Hidden Nucleus of IC 5063 with NICMOS", Astrophysical Journal Letters, 492, L121 (1998).

[18] McCabe, C., Duchene, G., Ghez, A. M., "NICMOS Images of the GG Tauri Circumbinary Disk", Astrophysical Journal, 575, 974 (2002)

[19] Mathieu, R.D., "Pre-main-sequence binary stars." Annual Reviews of Astronomy and Astrophysics, 32, 465 (1994).

[20] Marsh, K.A., Silverstone, M.D., Becklin, E.E., Koerner, D.W., Werner, M.W., Weinberger, A.J., Ressler, M.E., "Mid-Infrared Images of the Debris Disk around HD 141569", Astrophysical Journal, 573, 425 (2002)

[21] Matthews, K., Nakajima, T., Kulkarni, S.R., Oppenheimer, B.R., "Spectral Energy Distribution and Bolometric Luminosity of the Cool Brown Dwarf Gliese 229B" Astronomical Journal, 112, 1678 (1996).

[22] Millan-Gabet, R., Schloerb, F.P., Traub, W.A., "Spatially Resolved Circumstellar Structure of Herbig AE/BE Stars in the Near-Infrared", Astrophysical Journal, 546, 358 (2001).

[23] Monin, J.-L., Bouvier, J., "Disks in multiple systems: direct imaging of a nearly edge-on circumstellar disk in the young triple system HV Tau", Astronomy and Astrophysics, 356, L75 (2000).

[24] Monnier, J.D., Tuthill, P.G., Lopez, B., Cruzalebes, P., Danchi, W.C., Haniff, C.A., "The last gasps of VY CMa: Aperture synthesis and adaptive optics imagery", Astrophysical Journal, 512, 351 (1998).

[25] Nakajima, T., Oppenheimer, B.R., Kulkarni, S.R., Golimowski, D.A., Matthews, K., Durrance, S.T., "Discovery of a Cool Brown Dwarf", Nature, 378, 463 (1995).

[26] Oppenheimer, B.R., Kulkarni, S.R., Matthews, K., Van Kerkwijk, M.H., "The Spectrum of the Brown Dwarf Gliese 229B", Astrophysical Journal, 502, 932 (1998).

[27] Peterson, B.M., et al., "Steps toward determination of the size and structure of the broad-line region in active galactic nuclei. II - An intensive study of NGC 5548 at optical wavelengths" Astrophysical Journal, 368, 119 (1991).

[28] Reid, I.N., Gizis, J.E., "The Palomar/MSU Nearby Star Spectroscopic Survey.II. The Southern M Dwarfs and Investigation of Magnetic Activity", Astronomical Journal, 113, 2246 (1997).

[29] Reid I.N., Kirkpatrick D., Beichman C.A., Liebert J., Burrows A., Skrutskie M., "2MASS Brown Dwarfs and the Substellar Mass Function" Astronomy and Astrophysics Supplement Series, 192, 5517 (1998).

[30] Richards, A.M.S., Yates, J.A., " MERLIN observations of water maser proper motions in VY Canis Majoris", Monthly Notices of the Royal Astronomical Society, 299, 319 (1998).

[31] Schreier, E.J., et al., "Evidence for a 20pc Disk at the Nucleus of Centaurus A", Astrophysical Journal Letters, 499, L143 (1998).

[32] Shu, F., Najita, J., Ostriker, E., Wilkin, F., Ruden, S., Lizano, S., "Magneto-centrifugally driven flows from young stars and disks. 1: A generalised model", Astrophysical Journal, 429, 781 (1994).

[33] Simon, M., Ghez, A.M., Leinert, C.H., Cassar, L., Chen, W. P., Howell, R.R., Jameson, R.F., Matthews, K., Neugebauer, G., Richichi, A., "A lunar occultation and direct imaging survey of multiplicity in the Ophiuchus and Taurus star-forming regions", Astrophysical Journal, 443, 625 (1995).

[34] Spitzer, L. Diffuse Matter in Space, New York: Interscience (1968).

[35] Tuthill, P.G., Haniff, C.A., Baldwin, J.E. "Hotspots on late-type Supergiants", Monthly Notices of the Royal Astronomical Society, 285, 529 (1997).

[36] Uzdensky, D., Konigl, A., Litwin, C., "Magnetically Linked Star-Disk Systems. I. Force-free Magnetospheres and Effects of Disk Resistivity", Astrophysical Journal, 565, 1191 (2002).

[37] van der Kruit, P. C. & Allen, R. J., Annual Reviews of Astronomy and Astrophysics, 16, 103 (1978).

[38] Weinberger A.J., Becklin E.E., Schneider G., Smith, B.A., Lowrance P.J., Silverstone M.D., Zuckerman B., Terrile, R.J., "The Circumstellar Disk of HD 141569 Imaged with NICMOS", Astrophysical Journal, 525, 53L (1999)